Towards a self-consistent theory of pulsar magnetospheric HE/VHE emissions

HIROTANI, Kouichi

ASIAA/TIARA, Taiwan

Nagoya University
July 26, 2013

Crab nebula: Composite image of X-ray [blue] and optical [red]

§1 γ-ray Pulsar Observations

After 2008, LAT aboard Fermi has detected more than 117 pulsars above 100 MeV.

Fermi/LAT point sources (>100 MeV)

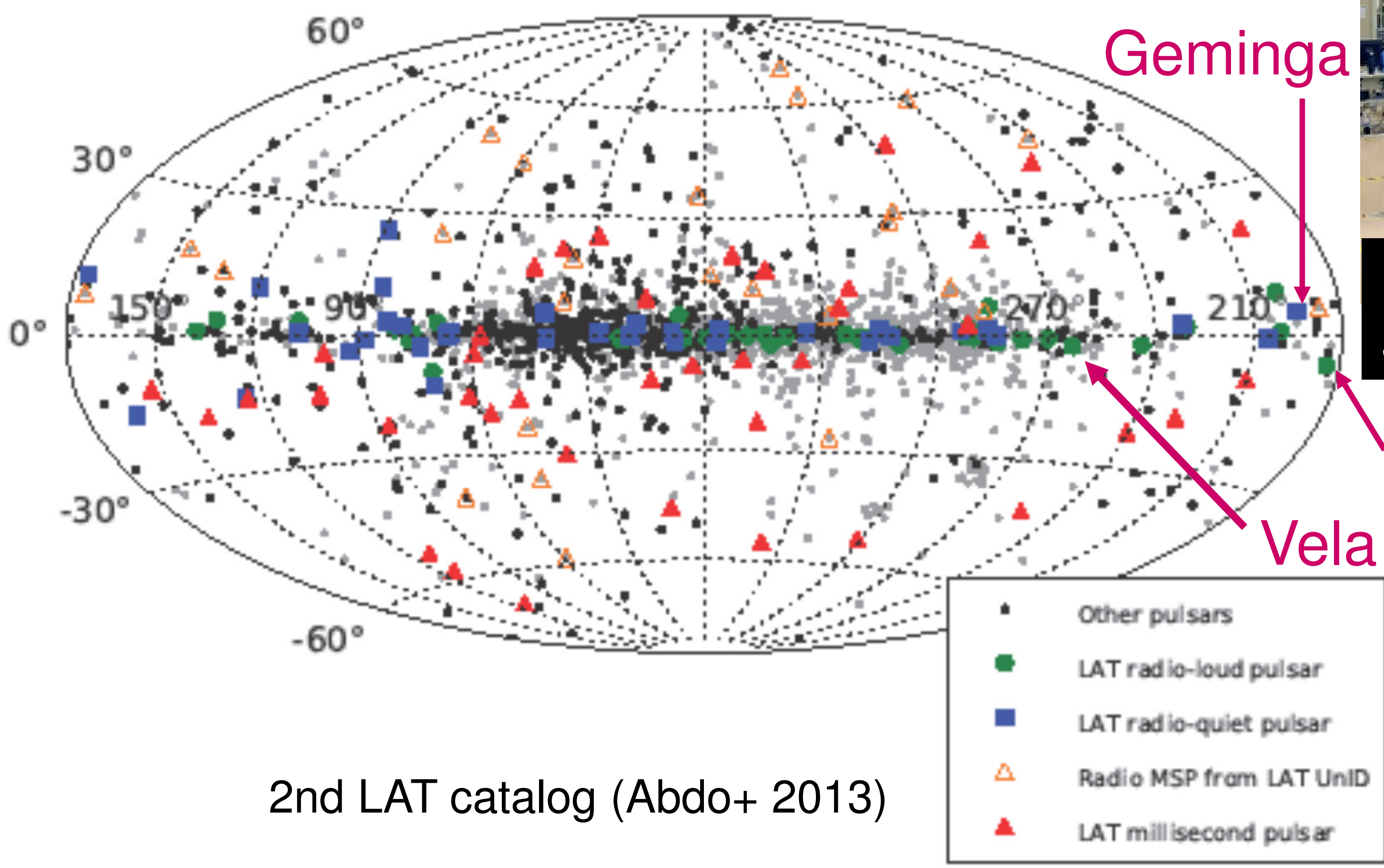

2nd LAT catalog (Abdo+ 2013)

Large Area Telescope

Fermi γ-ray space telescope

§1 γ-ray Pulsar Observations

Ground-based, Imaging Air Cherenkov Telescopes (IACTs) found pulsed emission above 25 GeV from the Crab pulsar.

VERITAS (> 120 GeV)

Aliu+ (2011, Science 334, 69)

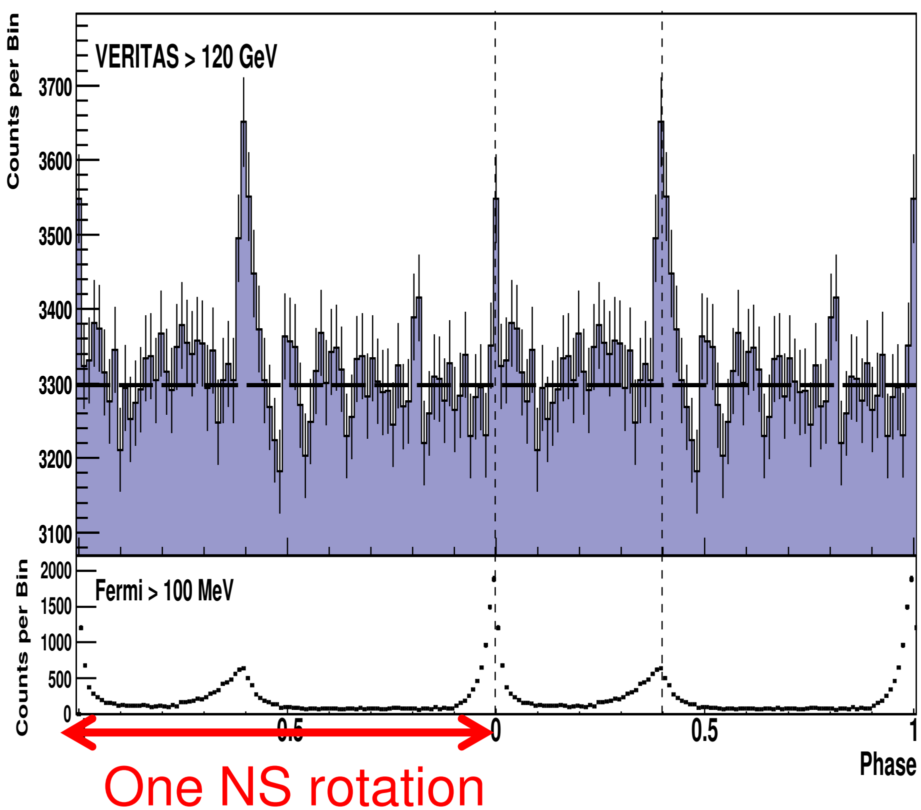

MAGIC (25−416 GeV)

Aleksić+ (2011a,b)

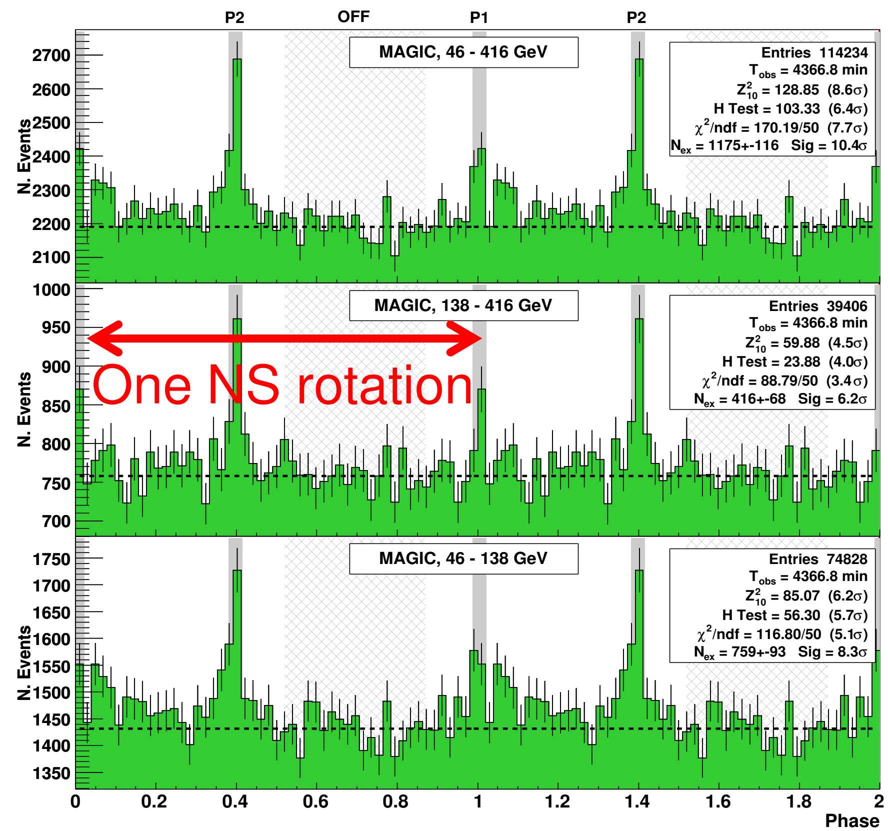

Pulsed broad-band spectra

- High-energy (~ GeV) photons are emitted mainly via **curvature** process by ultra-relativistic, primary e^{-}'s/e^{+}'s.

(created in the particle accelerator)

(Thompson, EGRET spectra)

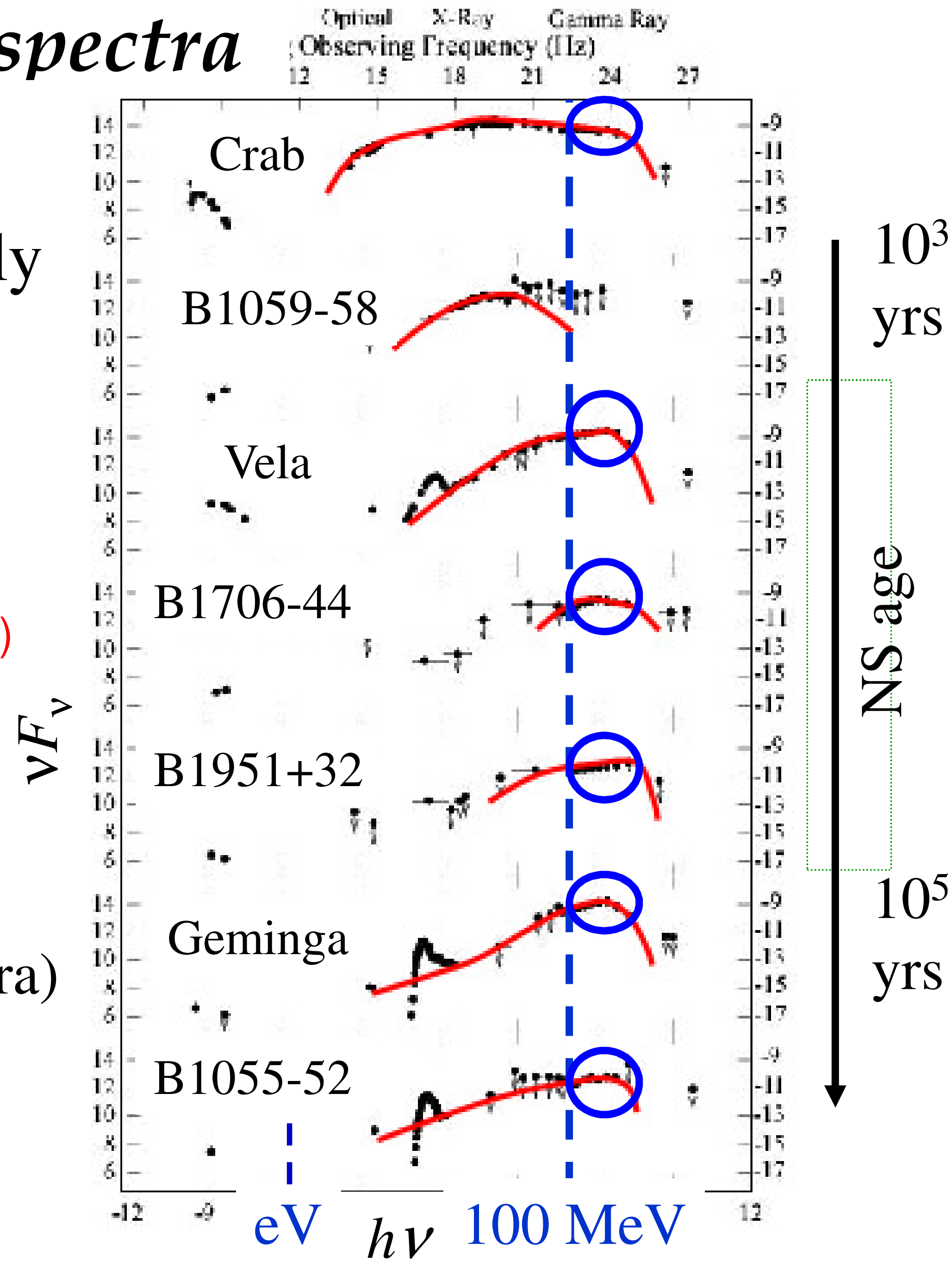

Pulsed broad-band spectra

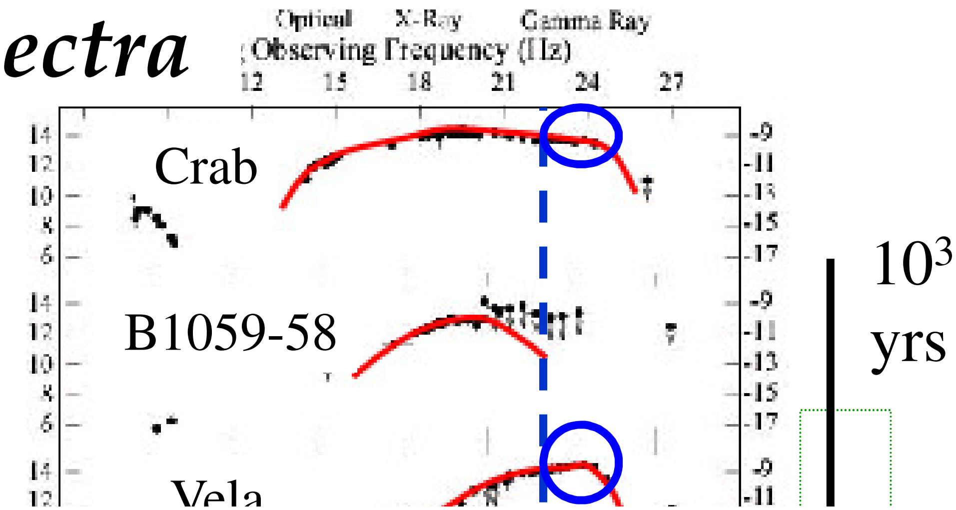

- High-energy (>100MeV) photons are emitted mainly via **curvature** process by ultra-relativistic $e^{\pm}$'s.

What is the curvature process?

Consider relativistic charges moving along curved ***B***. They emit curvature radiation, provided $P_{||} \gg P_{\perp}$. A charge e with Lorentz factor γ emits the following synchrotron radiation,

cf. synchrotron case

characteristic energy: $\hbar\omega_{\rm curv} = \frac{3}{2}\hbar\gamma^3\frac{c}{R_{\rm c}}$ $\qquad \hbar\omega_{\rm c} = \frac{3}{2}\hbar\gamma^3\frac{c}{r_{\rm g}}$

radiation power: $P_{\rm curv} = \frac{3e^2}{2c^3}\gamma^4\left(\frac{c^2}{R_{\rm c}}\right)^2$ $\qquad P_{\rm synch} = \frac{3e^2}{2c^3}\gamma^4\left(\frac{c^2}{r_{\rm g}}\right)^2$

Pulsed broad-band spectra

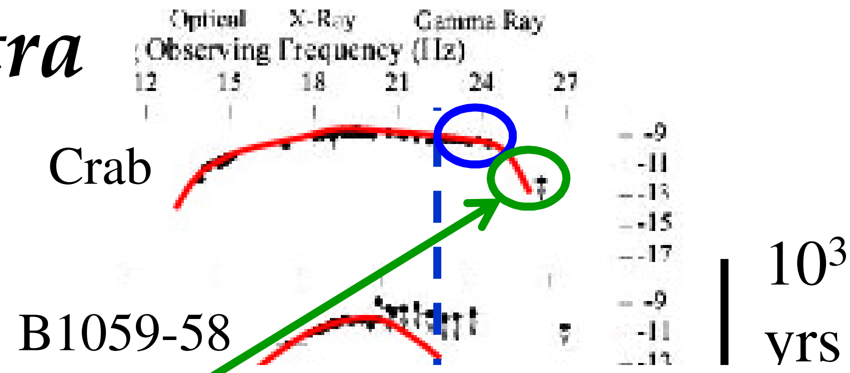

- High-energy (>100MeV) photons are emitted mainly via **curvature** process by ultra-relativistic, primary $e^{\pm}$'s.

- However, > 20 GeV, **ICS by secondary & tertiary $e^{\pm}$'s** contributes.

For pulsar VHE emissions, Klein-Nishina effect becomes important, because $\varepsilon^*_{\rm i} \gg m_{\rm e}c^2$.

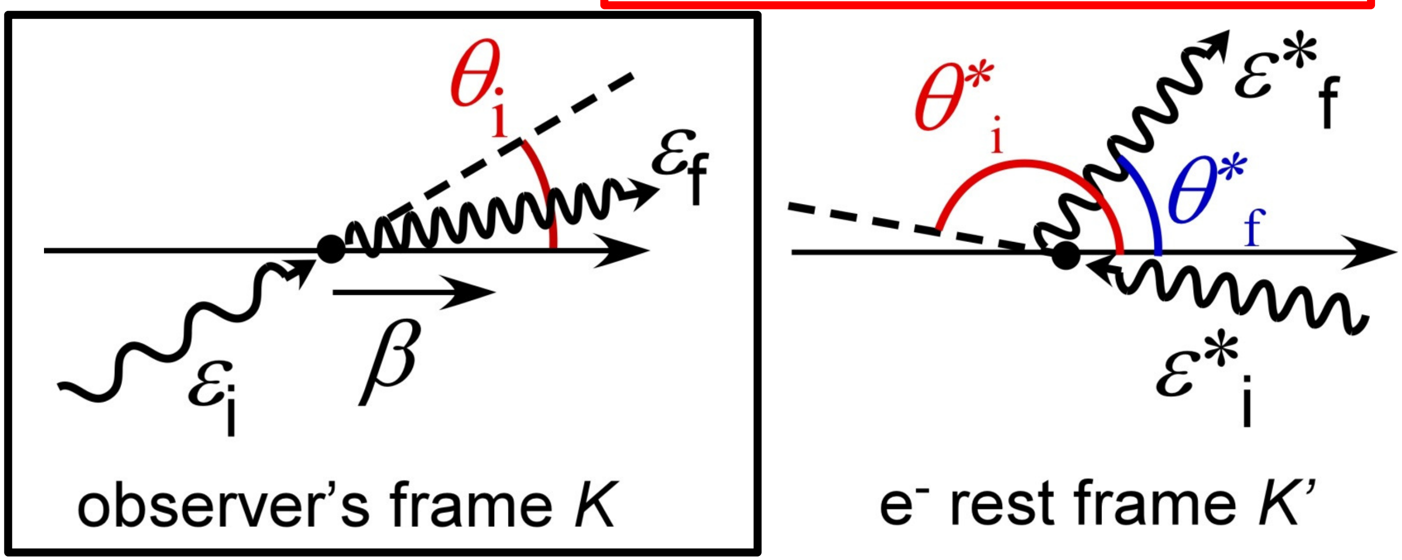

Fig. Two Lorentz frames when a photon is up-scattered by a relativisitic e^-.

§2 Pulsar Emission Models

Let us begin with considering how and where such incoherent, high-energy photons are emitted from pulsars.

§2 Pulsar Emission Models

High-energy emissions are realized when the rotational energy of the NS is electro-dynamically extracted and partly dissipated in the magnetosphere. (e.g., unipolar inductor)

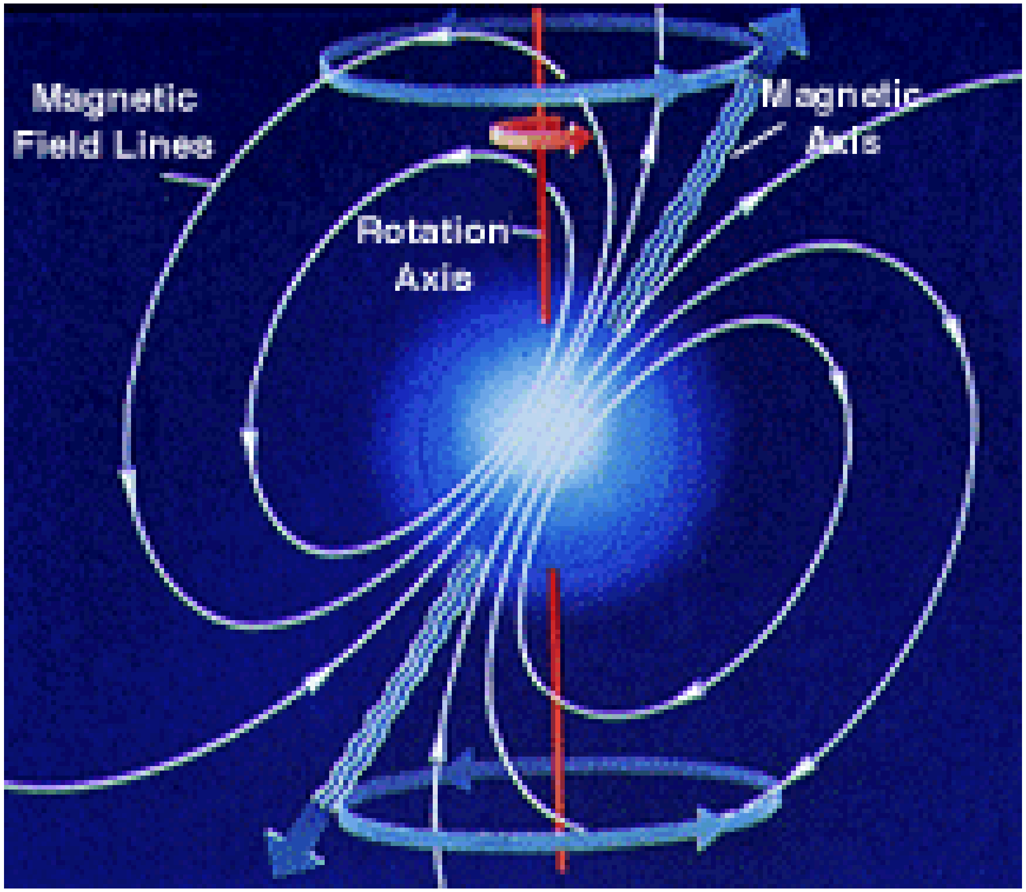

Magnetic and rotation axes are generally misaligned.

Pulsars:

rapidly rotating, highly magnetized NS

§2 Pulsar Emission Models

Pulsar emission takes place at …

- Polar gap

  (r <30 km), near NS surface

- Outer gap, or slot gap

  (r ~10^3 km), near the light cylinder

  (outside the null surface)

- Wind region

  We neglect the emission from the wind region, because they are not pulsed.

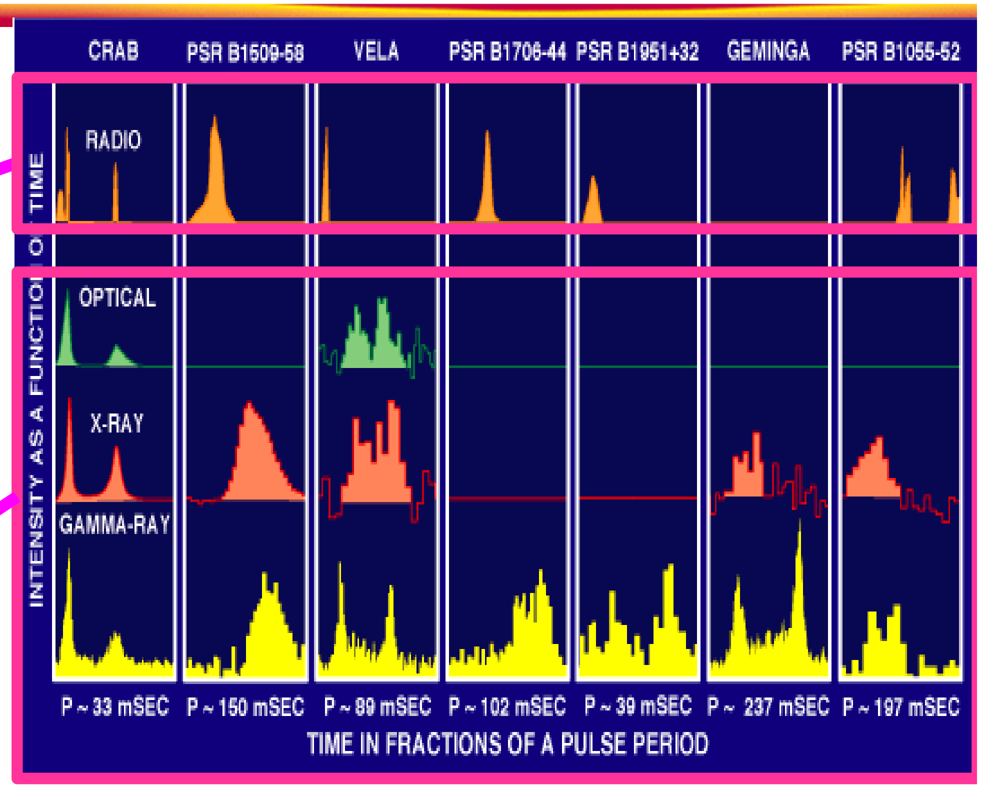

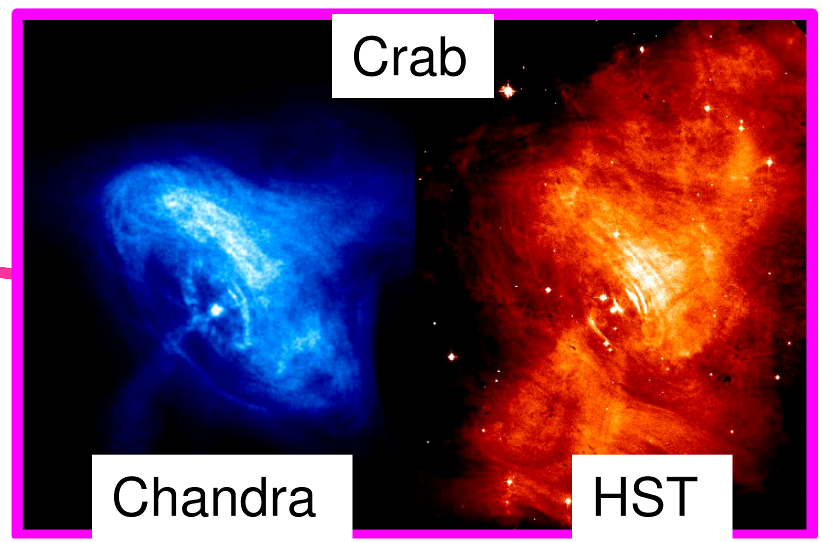

§2 Pulsar Emission Models

Pulsar emission takes place at …

- Polar gap
  (r <30 km), near NS surface

$E_{\parallel}$ arises in a limited volume near the PC surface due to heavy screening by pair discharge.

- Outer gap, or slot gap
  (r ~10^3 km), near the light cylinder
  (outside the null surface)

$E_{\parallel}$ arises in a greater volume in the higher altitudes due to less efficient pair production.

§2 *Pulsar Emission Models*

Early 80's, the polar-cap (PC) model was proposed.

(Daugherty & Harding ApJ 252, 337, 1982)

A single PC beam can produce a variety of pulse profiles.

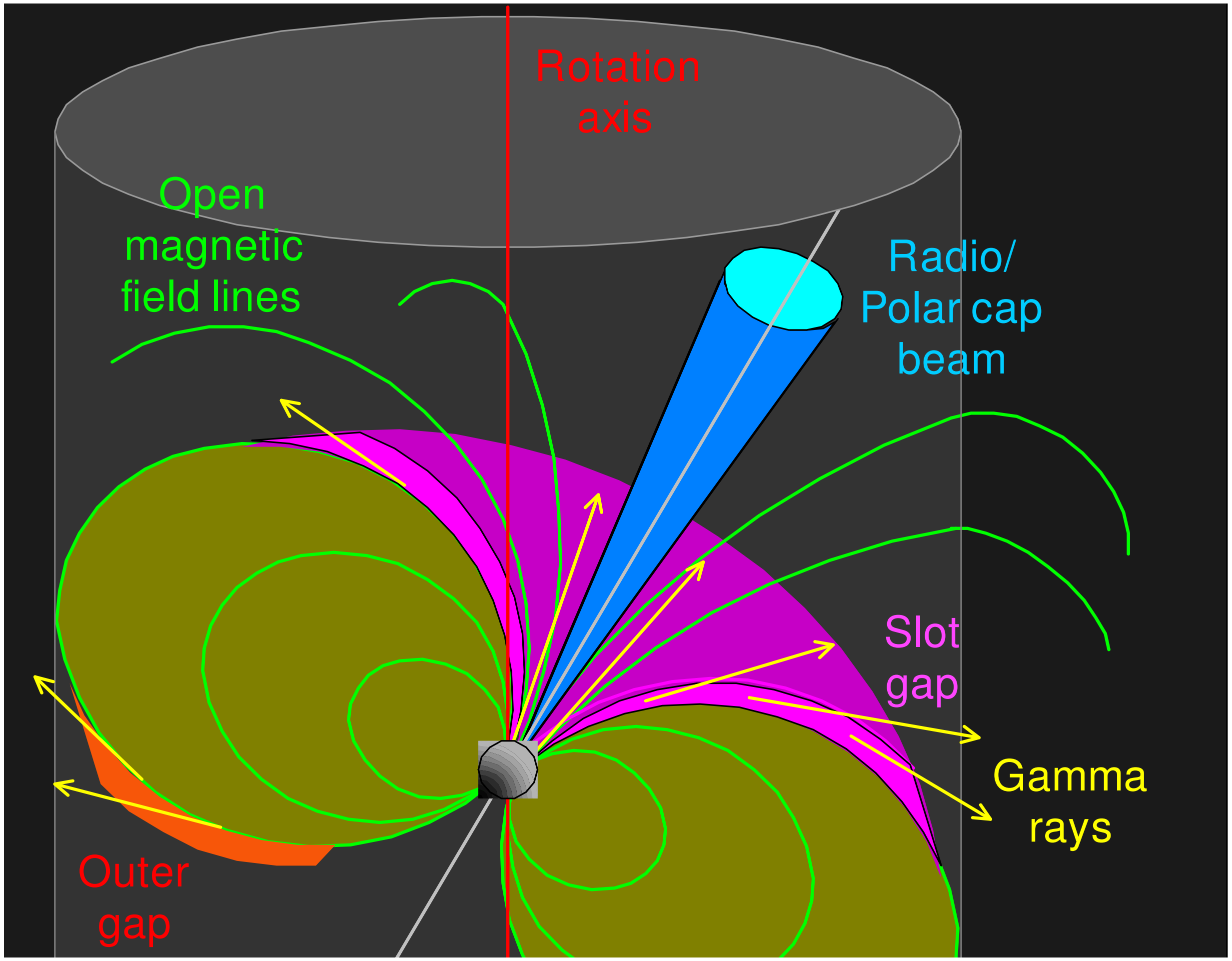

§2 Pulsar Emission Models

Early 80's, the polar-cap (PC) model was proposed.
(Daugherty & Harding ApJ 252, 337, 1982)

A single PC beam can produce a variety of pulse profiles.

However, the emission solid angle ($\Delta\Omega$ «1 ster) was too small to reproduce the wide-separated double peaks.

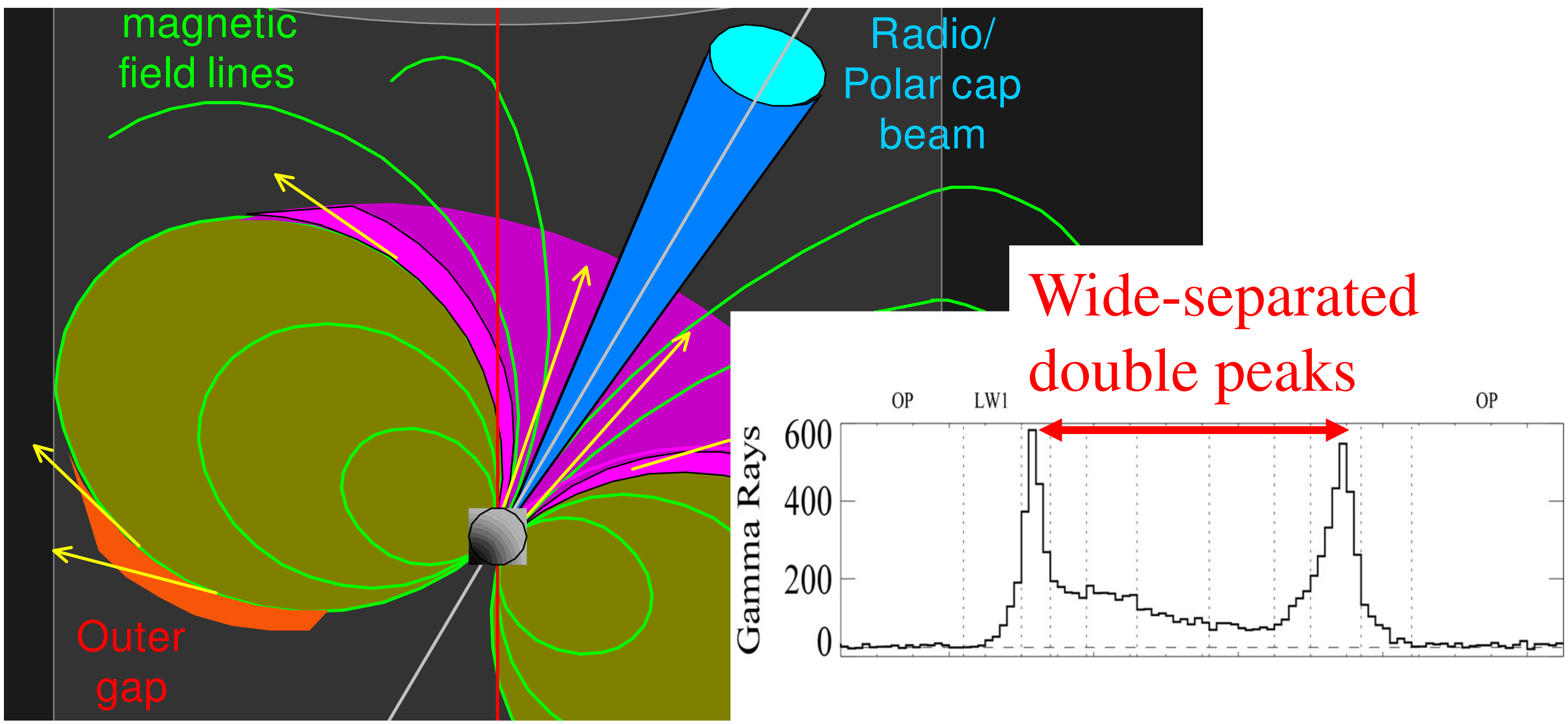

§2 *Pulsar Emission Models*

Early 80's, the polar-cap (PC) model was proposed.

(Daugherty & Harding ApJ 252, 337, 1982)

A single PC beam can produce a variety of pulse profiles.

However, the emission solid angle ($\Delta\Omega \ll 1$ ster) was too small to reproduce the wide-separated double peaks.

Thus, a high-altitude emission drew attention.

§2 Pulsar Emission Models

To contrive a higher-altitude emission model, the polar gap was extended into higher altitudes (in fact, by hand).

Muslimov & Harding (2004a, ApJ 606, 1143;
2004b, ApJ 617, 471)
Dyks, Harding & Rudak (2004, ApJ 606, 1125)
Harding+ (2008, ApJ ApJ 680, 1378)

They explained, e.g., the widely separated double peaks.

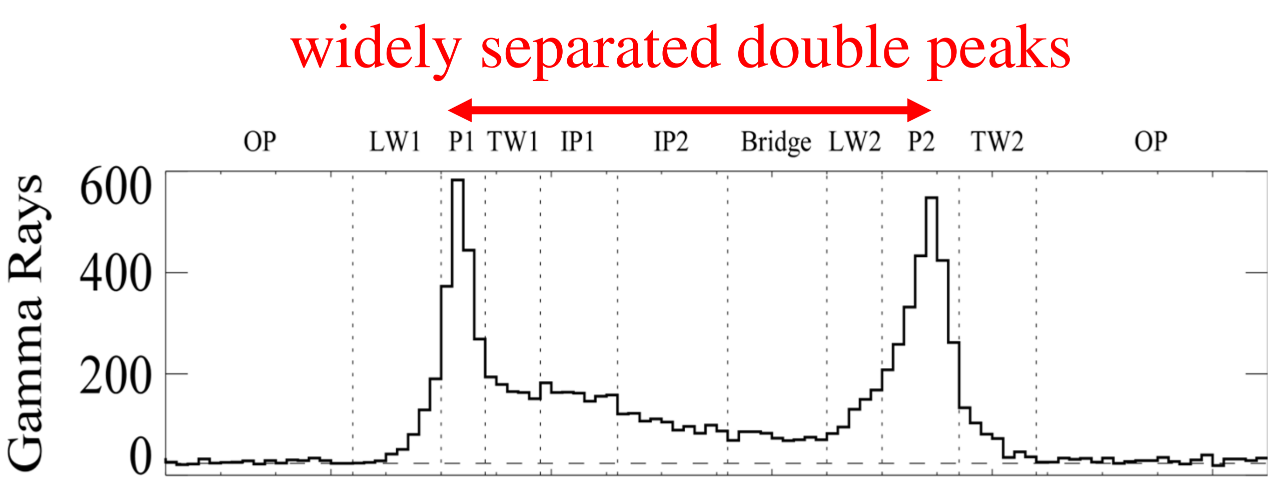

§2 Pulsar Emission Models

To contrive a higher-altitude emission model, the polar gap was extended into higher altitudes (in fact, by hand).

Muslimov & Harding (2004a, ApJ 606, 1143;
2004b, ApJ 617, 471)
Dyks, Harding & Rudak (2004, ApJ 606, 1125)
Harding+ (2008, ApJ ApJ 680, 1378)

They explained, e.g., the widely separated double peaks.

However, unfortunately, the higher-altitude SG model contains two fatal electro-dynamical inconsistencies.

§2 *Pulsar Emission Models*

Problem 1: insufficient luminosity

This numerical conclusion is confirmed also analytically (KH'08), showing that **a SG can produce only a negligible γ-ray flux.**

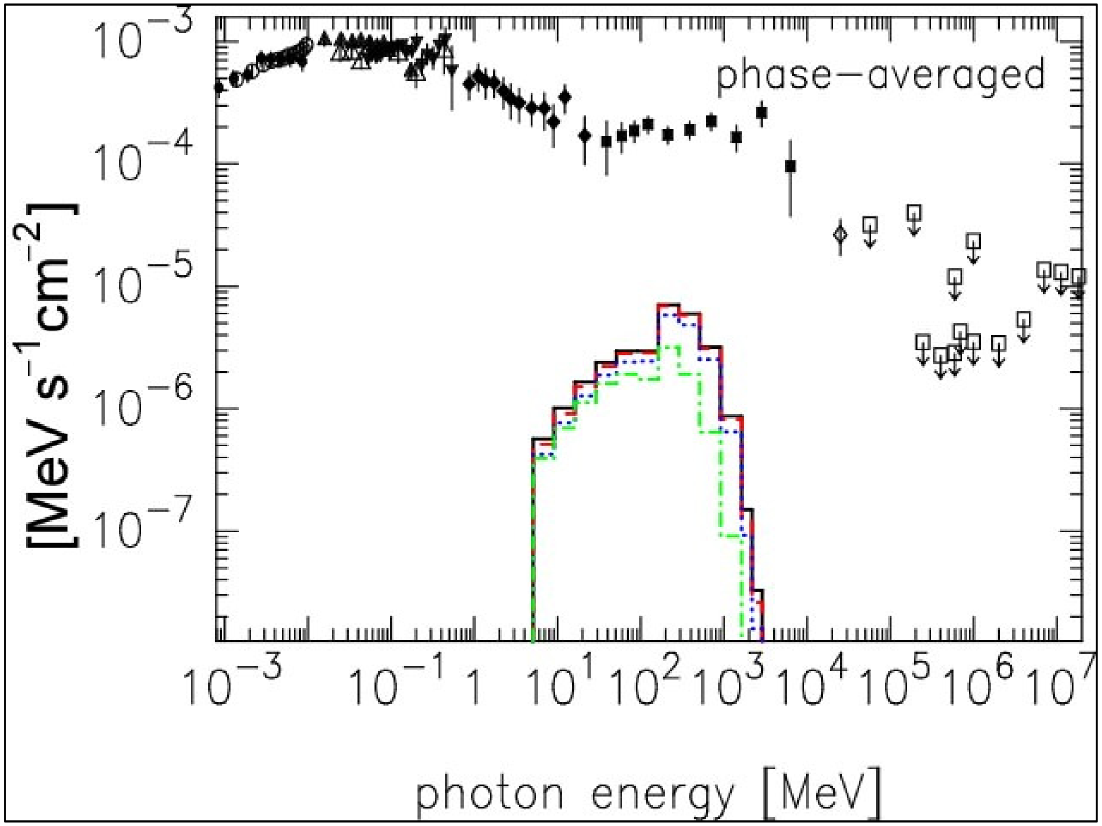

For details, please also refer to my talk last year at CTA-Japan meeting.

KH (2008) ApJ 688, L25

Problem #2: unphysical assumption of ρ_{GJ}/B

In the SG model, they assume ρ_{GJ}/B distribution that contradicts with the Maxwell equation.

For details, please also refer to my talk last year at CTA-Japan meeting.

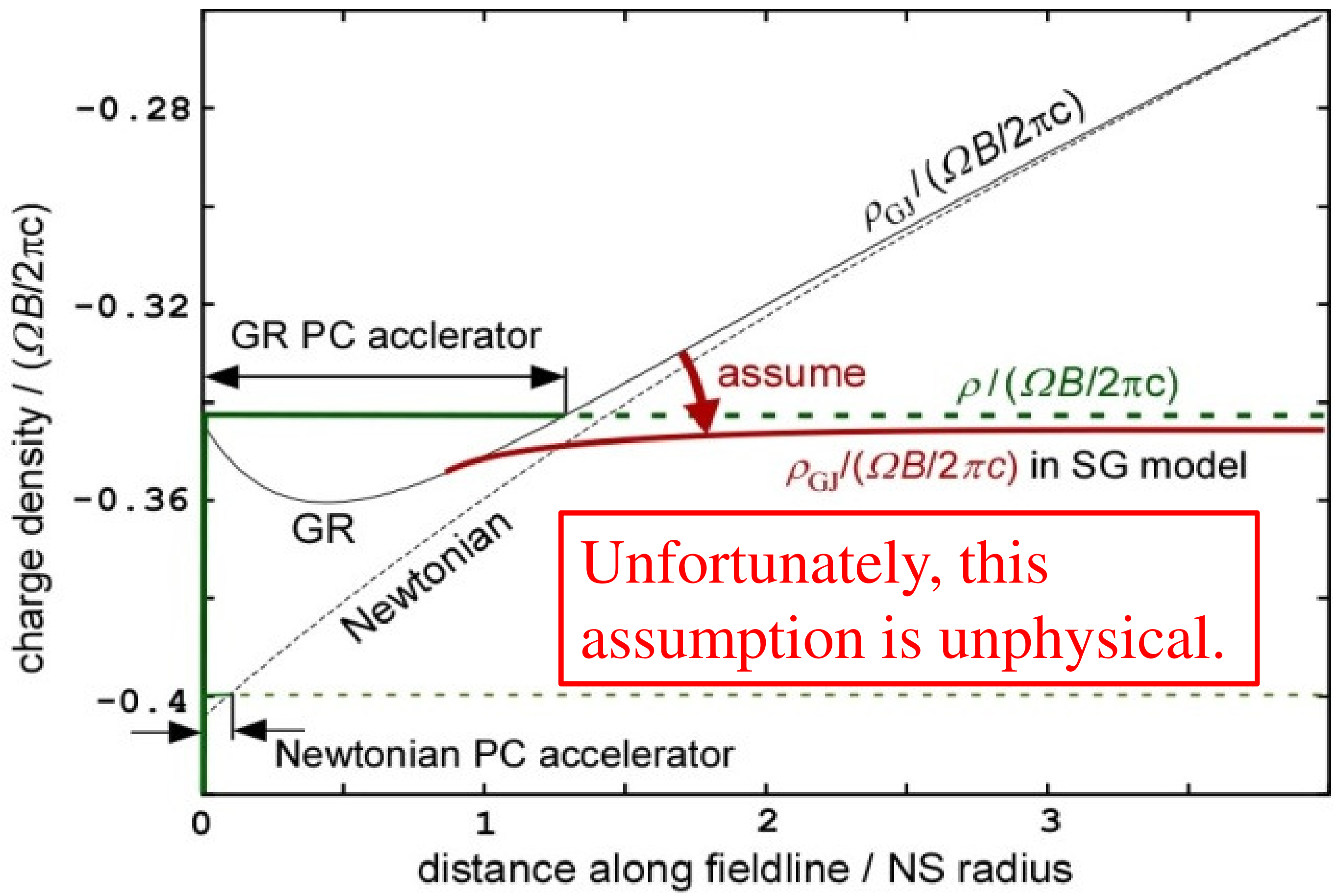

Problem #2: unphysical assumption of $\rho_{\mathrm{GJ}}/\mathrm{B}$

In fact, to solve the insufficient flux problem (prob. #1), a geometrically thick version of the higher-altitude SG model, the pair-starved PC (PSPC) model, was proposed (Venter+ 2009, ApJ 707, 800). However, the PSPC model adopts the same ρ_{GJ}/B distribution, which means that the same difficulty applies.

Higher-latitude SG model & PSPC model contradict with Maxwell eq. That is, higher-altitude extension of the polar-cap model failed.

§2 Pulsar Emission Models

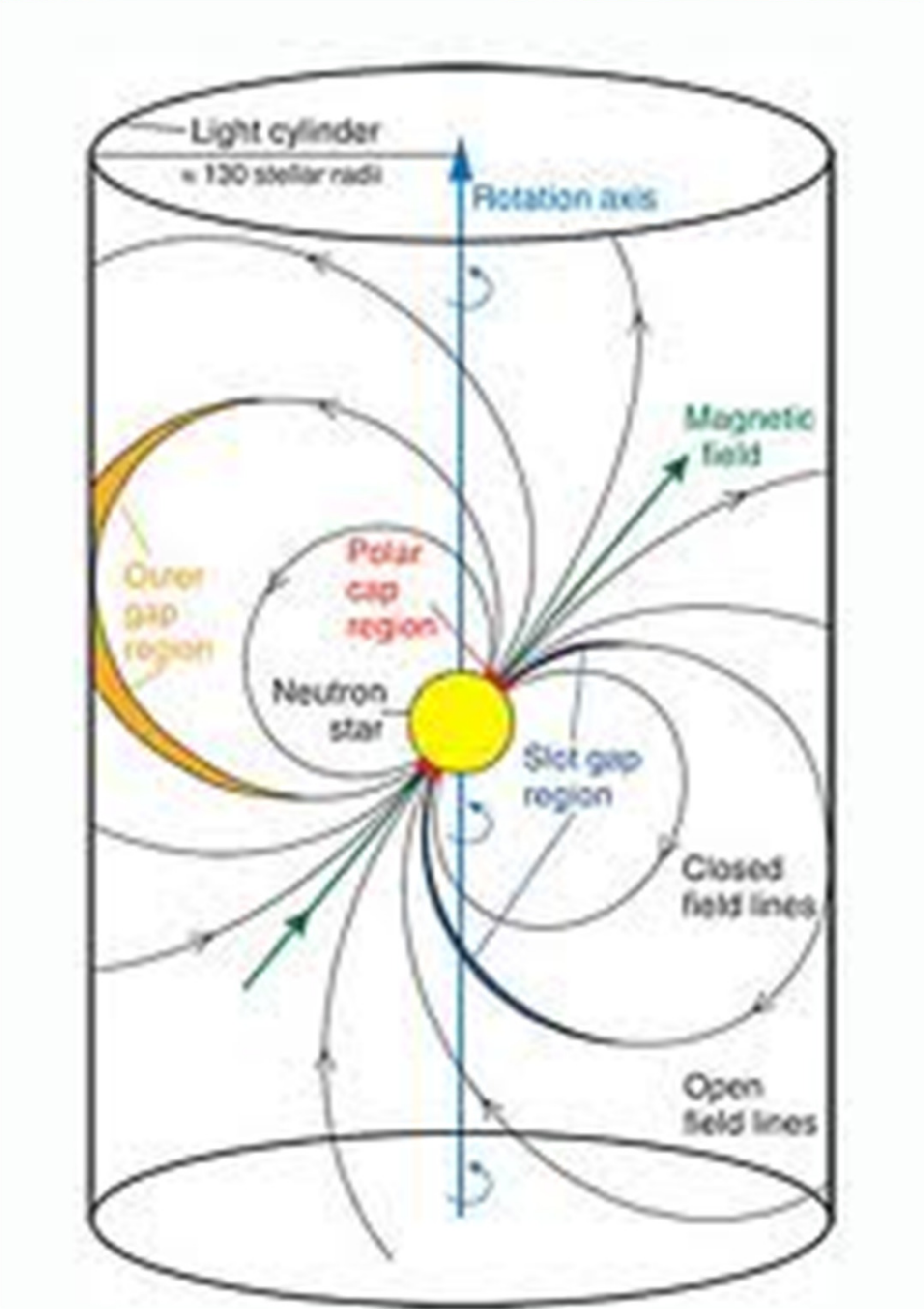

As an alternative possibility of high-altitude emission model, the outer gap model was proposed.

Cheng, Ho, Ruderman (1986, ApJ 300, 500)

So far, there have been found no serious electro-dynamical problems in the OG model (unlike SG or PSPC model).

Thus, let us concentrate on the OG model in what follows.

§2 Pulsar Emission Models

Indeed, the sub-TeV components from the Crab pulsar shows that pulsed γ-rays are emitted from the **outer** magnetosphere (~~$\gamma B \to ee$~~).

We thus consider the outer-gap model (Cheng+ 86, ApJ 300,500) in this talk.

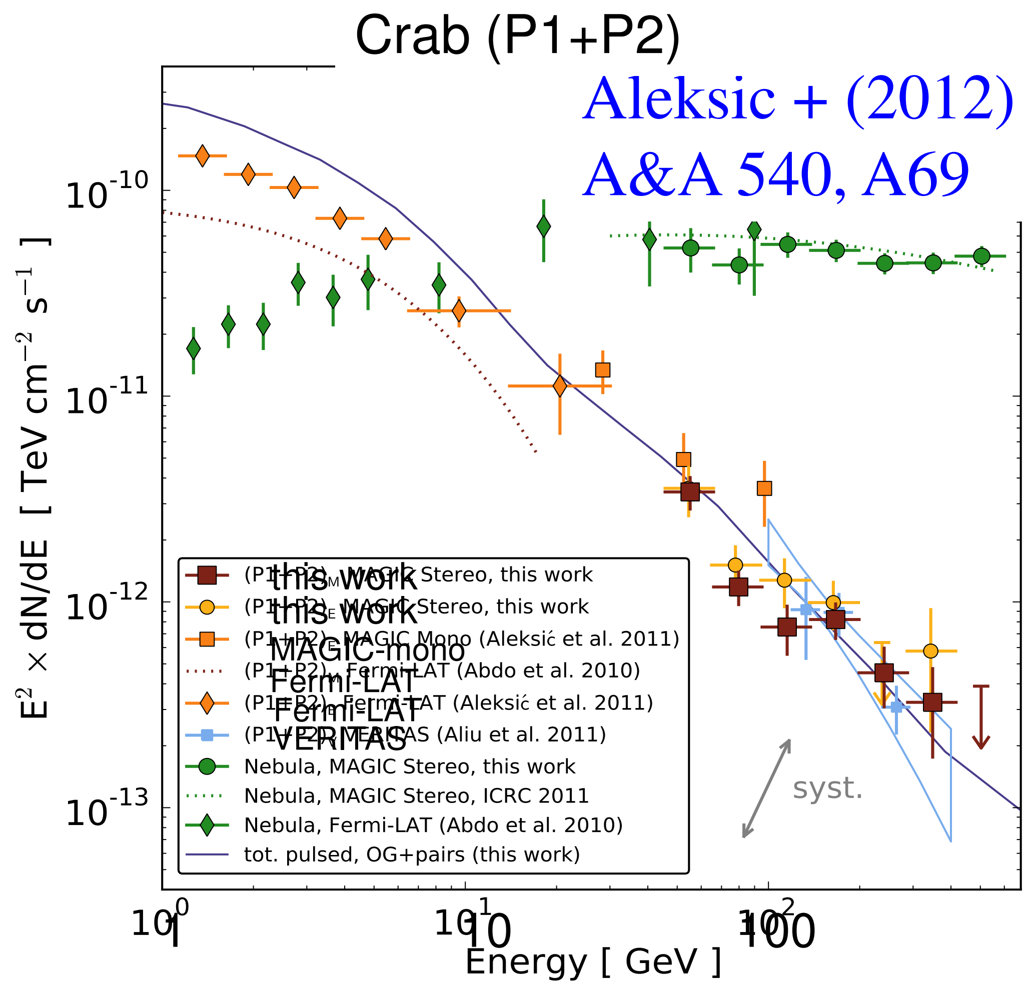

Aleksic + (2012)
A&A 540, A69

§2 *Pulsar Emission Models*

Various attempts have been made on recent OG model:

3-D geometrical model

→ phase-resolved spectra (Cheng + ’00; Tang + ’08)

→ atlas of light curves for PC, OG, SG models (Watters + ’08)

2-D self-consistent solution (Takata + ’06; KH ’06)

3-D self-consistent solution

→ phase-resolved spectra, absolute luminosity if we give only P, dP/dt, α, kT $(+\zeta)$ (this talk)

In this talk, I’ll present the most recent results obtained in my 3-D version of self-consistent OG calculations.

§2 *Pulsar Emission Models*

3-D self-consistent OG model

Death line of normal and millisecond PSRs on $(P, \dot{P})$ plane

(Wang & KH 2011, ApJ 736, 127)

Spectral hardening of trailing light-curve peak

(KH 2011, ApJ 733, L49)

Evolution of γ-ray luminosity of rotation-powered PSRs

(KH 2013, ApJ 766, 98)

Today's talk I.

Today's talk II.

Crab pulsars HE-VHE pulsed emission

(Alkesic + 2011, ApJ 742, 43; Alkesic + 2012, AA 540, A69)

Comment on Lorentz invariance violation tests.

§3 Modern Outer-gap Model: Formalism

Self-sustained pair-production cascade in a rotating NS magnetosphere:

$e^{\pm}$'s are accelerated by $E_{||}$

↓

Relativistic e^+/e^- emit γ-rays via synchro-curvature, and IC processes

↓

γ-rays collide with soft photons/B to materialize as pairs in the accelerator

§3 Modern OG Model: Formalism

Poisson equation for electrostatic potential ψ :

$$-\nabla^2\psi = -\frac{\partial^2\psi}{\partial x^2} - \frac{\partial^2\psi}{\partial y^2} - \frac{\partial^2\psi}{\partial z^2} = 4\pi(\rho - \rho_{\rm GJ}) \ ,$$

where

$$E_{||} \equiv -\frac{\partial\psi}{\partial x} \ , \ \rho_{\rm GJ} \equiv -\frac{\mathbf{\Omega}\bullet\mathbf{B}}{2\pi c},$$

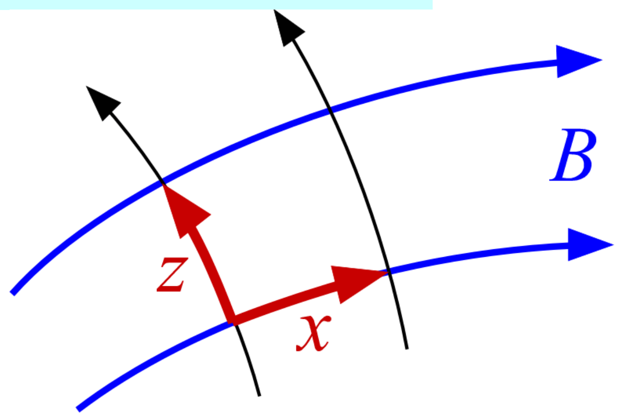

$$\rho(\mathbf{x}) \equiv e\int_1^\infty d\gamma \int_0^\pi d\chi \left[N_+(\mathbf{x},\gamma,\chi) - N_-(\mathbf{x},\gamma,\chi)\right] + \rho_{\rm ion}(\mathbf{x}),$$

$$\mathbf{x} = (x, y, z) \ .$$

N_+/N_-: distrib. func. of e^+/e^-

γ: Lorentz factor of e^+/e^-

χ : pitch angle of e^+/e^-

§3 Modern OG Model: Formalism

Assuming $\partial_t + \Omega\partial_\phi = 0$, we solve the $e^{\pm}$'s Boltzmann eqs.

$$\frac{\partial N_\pm}{\partial t} + \vec{v}\cdot\nabla N_\pm + \left(e\vec{E}_\parallel + \frac{\vec{v}}{c}\times\vec{B} \right)\cdot\frac{\partial N_\pm}{\partial \vec{p}} = S_{IC} + S_{SC} + \int \alpha_\nu d\nu \int \frac{I_\nu}{h\nu} d\omega$$

together with the radiative transfer equation,

$$\frac{dI_\nu}{dl} = -\alpha_\nu I_\nu + j_\nu$$

$N_\pm$: positronic/electronic spatial # density,
$E_\parallel$: mangnetic-field-aligned electric field,
S_{IC}: ICS re-distribution function, $d\omega$: solid angle element,
I_ν: specific intensity, l : path length along the ray
α_ν: absorption coefficient, j_ν: emission coefficient

§3 Modern OG Model: Formalism

Boundary Conditions

To solve the elliptic-type differential eq. (Poisson eq.), we impose

$$\Psi = 0 \qquad \text{at inner, lower, upper BDs}$$

$$\frac{\partial \Psi}{\partial x} = 0 \qquad \text{at outer BD}$$

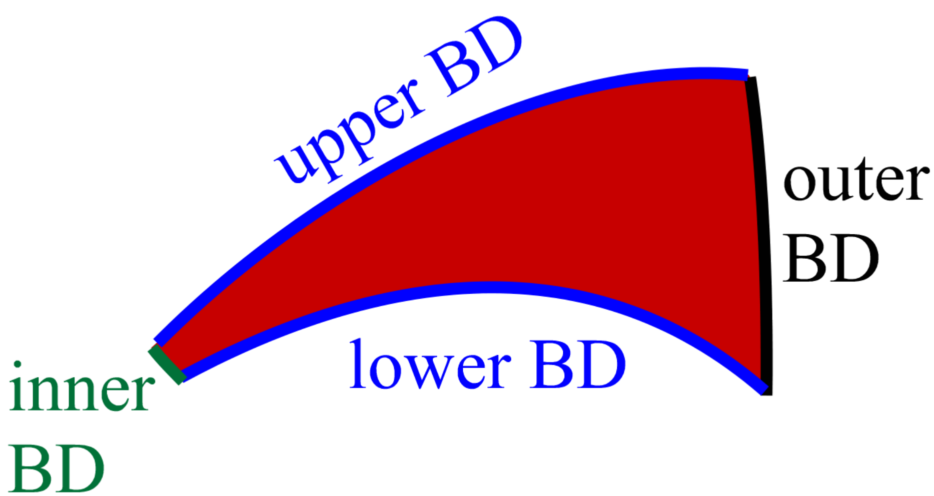

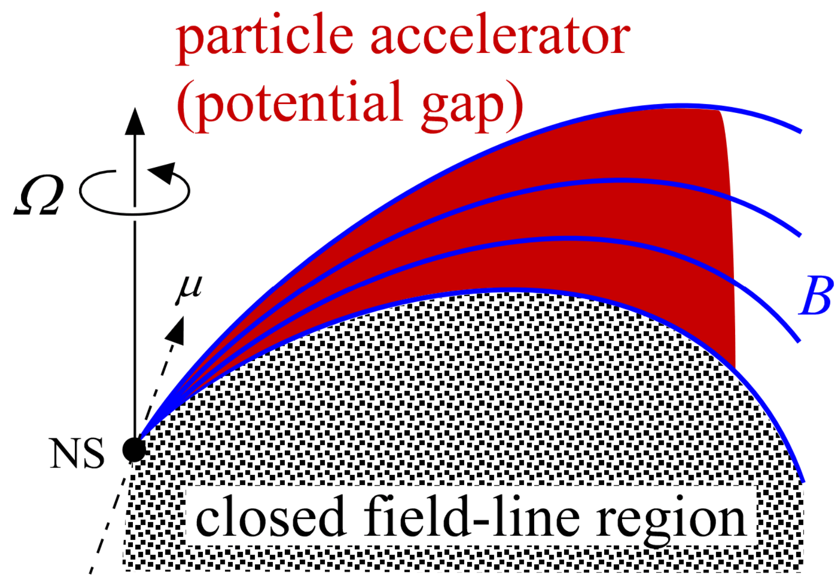

§3 Modern OG Model: Formalism

At the inner BD

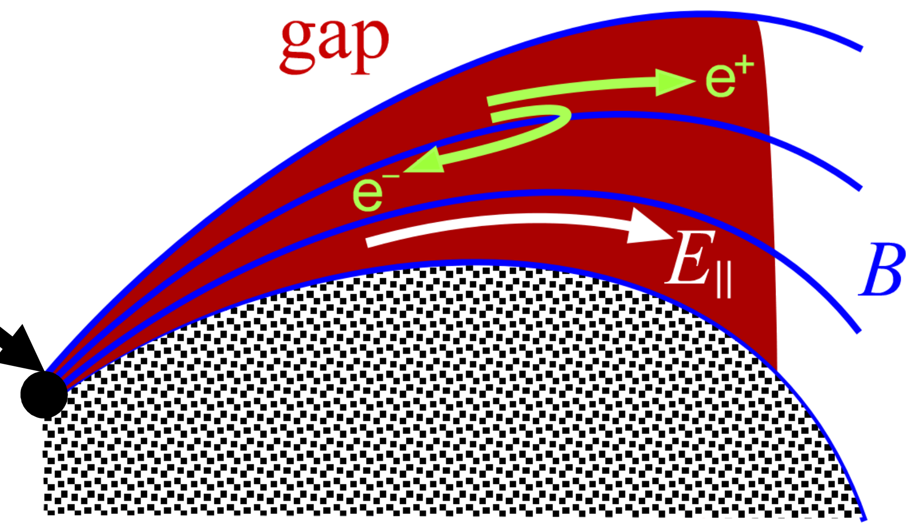

To solve the hyperbolic-type PDE ($e^{\pm}$ Boltzmann eq.), we impose

$$N_{+}(x^{\text{in}}, z, \gamma) = 0$$

To solve the ODE (radiative transfer eq.), we impose

$$I_{\nu}(x^{\text{in}}, z, \theta_{\gamma}) = 0, \quad \text{where } 0 < \theta_{\gamma} < \pi / 2 \text{ (outgoing)}$$

That is, no $e^{\pm}$/γ-ray injection across the BD.

§3 Modern OG Model: Formalism

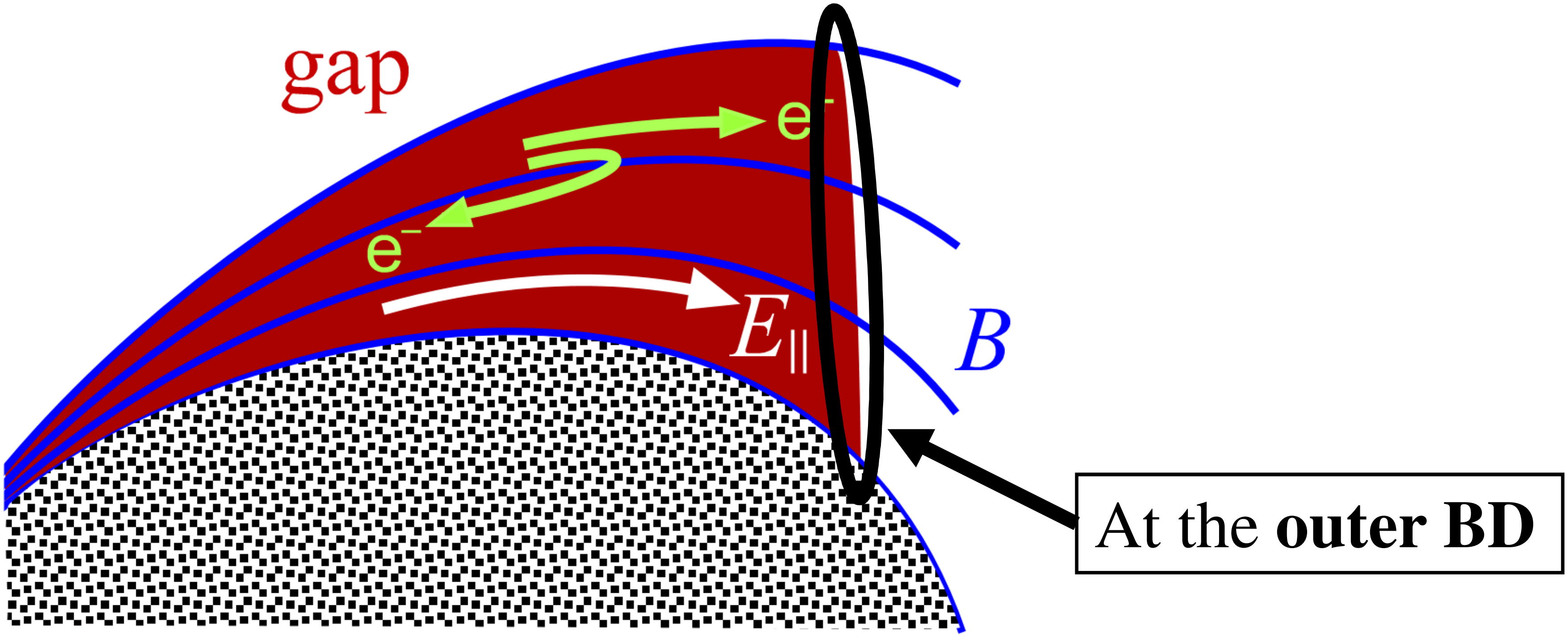

$$N_{-}(x^{\mathrm{out}}, z, \Gamma) = 0$$

$$I_{\nu}(x^{\mathrm{out}}, z, \theta_{\gamma}) = 0, \quad \text{where } \pi/2 < \theta_{\gamma} < \pi \text{ (in-going)}$$

That is, no $e^{\pm}$/γ-ray injection across the BD.

§4 Gamma-ray vs. Spin-down Luminosities

First, we demonstrate the observed $L_\gamma \propto L_{\rm spin}{}^{0.5}$.

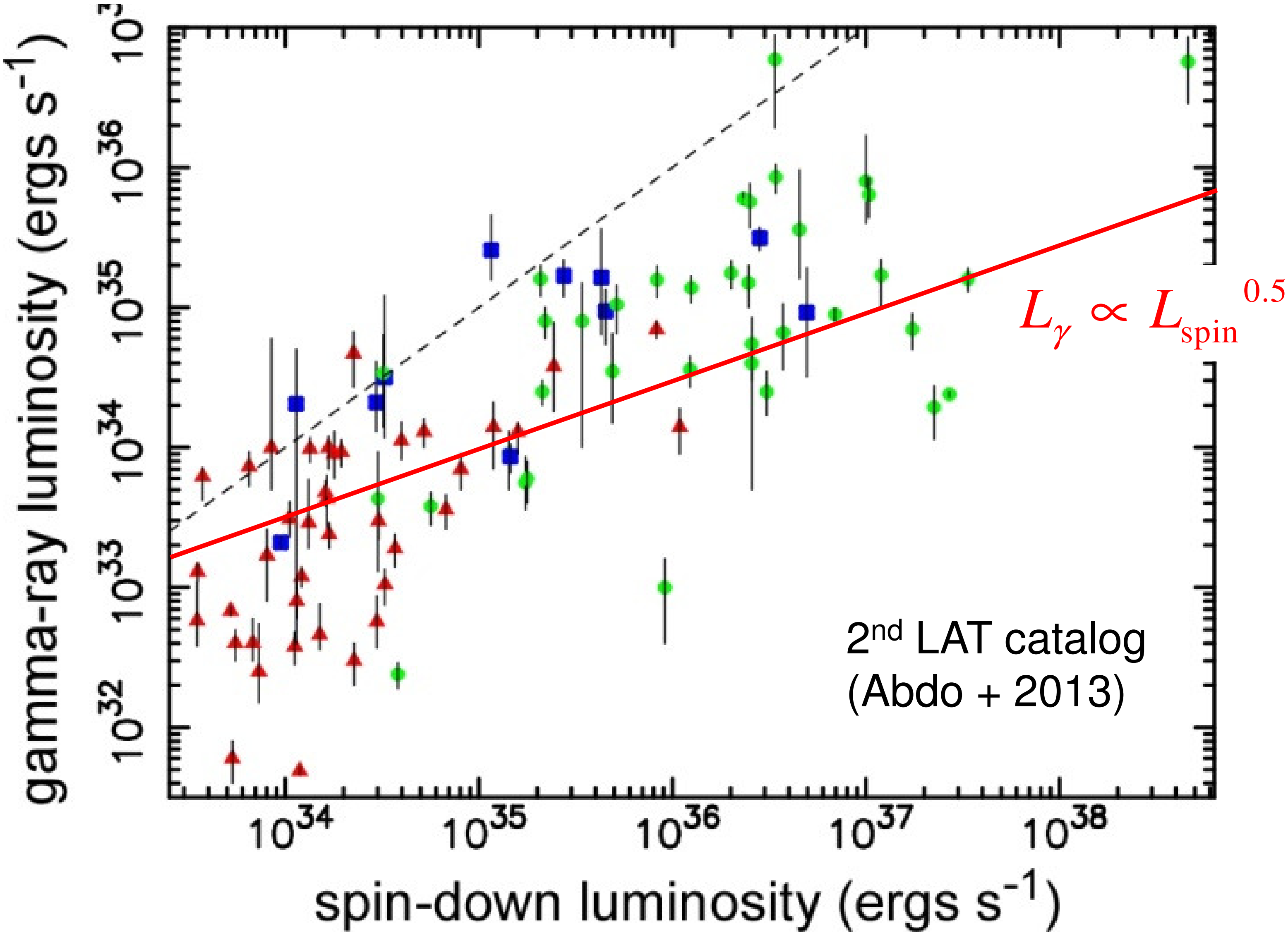

§4 Gamma-ray vs. Spin-down Luminosities

To begin with, let us analytically examine the condition for an OG to be self-sustained. An OG emits the energy flux (KH 2008, ApJ 688, L25)

$$(\nu F_\nu)_{\rm peak} \approx 0.0450 h_{\rm m}{}^3 \frac{\mu^2 \Omega^4}{c^3} \frac{1}{d^2},$$

at distance d by curvature process, where $h_{\rm m}$ denotes dimensionless OG trans-$\boldsymbol{B}$ thickness, μ the dipole moment.

OG luminosity can be, therefore, evaluated as

$$\mathrm{L}_\gamma \approx 2.36 (\nu F_\nu)_{\rm peak} \times 4\pi d^2 f_\Omega \approx 1.23 f_\Omega h_{\rm m}{}^3 \underbrace{\frac{\mu^2 \Omega^4}{c^3}}_{\propto \dot{E}}.$$

Thus, $h_{\rm m}$ controls the luminosity evolution.

§4 *Gamma-ray vs. Spin-down Luminosities*

To examine h_m, consider the condition of self-sustained OG.

An inward e^- emits N_γ^{in}~10^4 synchro-curvature photons, $N_\gamma^{in}\tau^{in}$~10 of which materialize as pairs.

Each returned, outward e^+ emits N_γ^{out}~10^5 curvature photons, $N_\gamma^{out}\tau^{out}$~0.1 of which materialize as pairs.

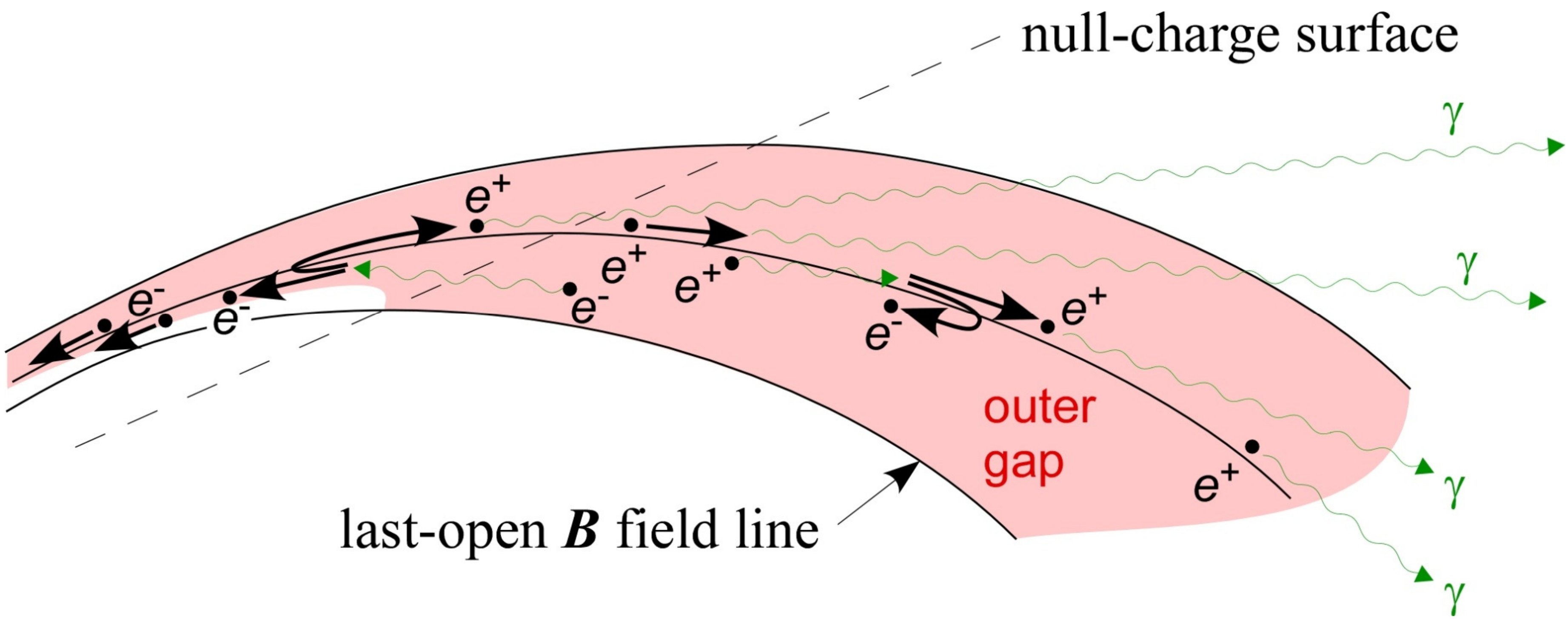

§4 *Gamma-ray vs. Spin-down Luminosities*

To examine h_m, consider the condition of self-sustained OG.

An inward e^- emits N_γ^{in}~10^4 synchro-curvature photons, $N_\gamma^{in}\tau^{in}$~10 of which materialize as pairs.

Each returned, outward e^+ emits N_γ^{out}~10^5 curvature photons, $N_\gamma^{out}\tau^{out}$~0.1 of which materialize as pairs.

That is, gap trans-***B***-field thickness h_m is automatically regulated so that $N_\gamma^{in}\tau^{in} N_\gamma^{out}\tau^{out}=1$ is satisfied.

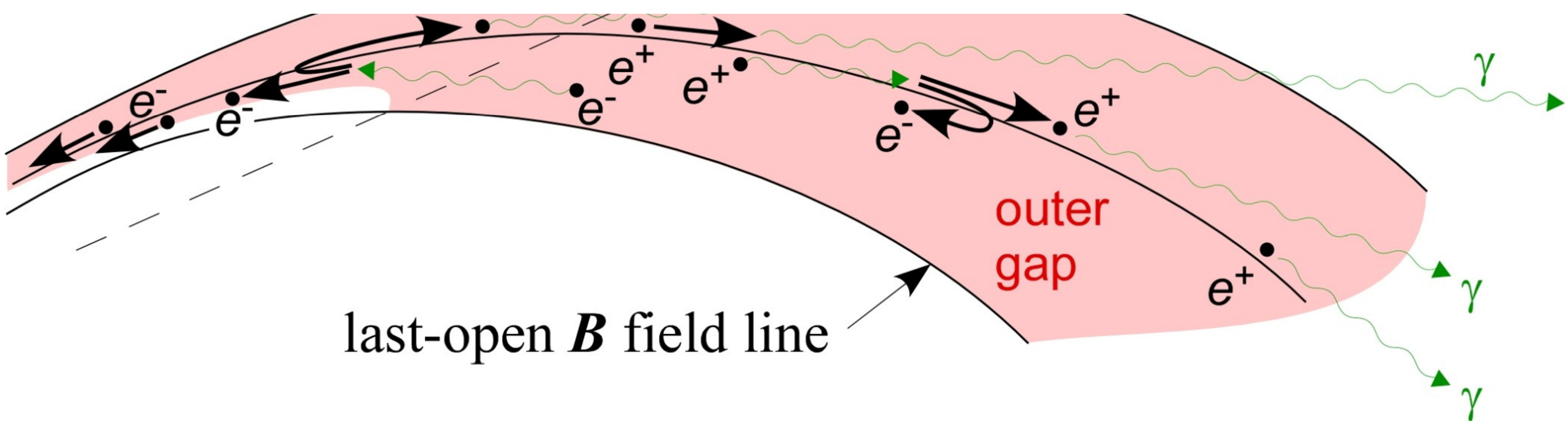

§4 Gamma-ray vs. Spin-down Luminosities

Step 1: Both $N_\gamma^{\rm in}\tau^{\rm in}$ and $N_\gamma^{\rm out}\tau^{\rm out}$ are expressed in terms of P, μ, α, T, and $h_{\rm m}$. Thus, $N_\gamma^{\rm in}\tau^{\rm in} N_\gamma^{\rm out}\tau^{\rm out}=1$ gives $h_{\rm m} = h_{\rm m}(P, \mu, \alpha, T)$.

That is, gap trans-***B***-field thickness $h_{\rm m}$ is automatically regulated so that $N_\gamma^{\rm in}\tau^{\rm in} N_\gamma^{\rm out}\tau^{\rm out}=1$ is satisfied.

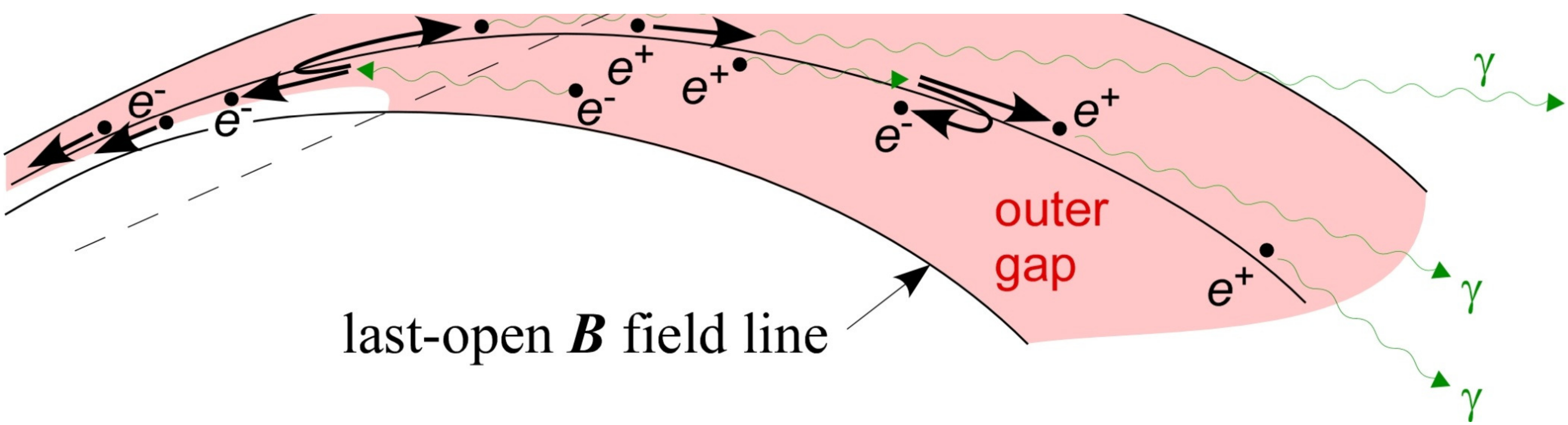

§4 *Gamma-ray vs. Spin-down Luminosities*

Step 1: express $N_\gamma^{\mathrm{in}}\tau^{\mathrm{in}}$ and $N_\gamma^{\mathrm{out}}\tau^{\mathrm{out}}$ with P, μ, α, T, h_{m}.

OG model predicts

$$E_{\|} \approx \frac{\mu}{2\varpi_{\mathrm{LC}}{}^3} h_{\mathrm{m}}{}^2 .$$

Particles ($e^{\pm}$'s) saturate at Lorentz factor,

$$\gamma = \left(\frac{3\rho_c^2}{2e} E_{\|} \right)^{1/4} ,$$

emitting curvature photons with characteristic energy,

$$h\nu_c = \frac{3}{2} \hbar c \frac{\gamma^3}{\rho_c} .$$

§4 *Gamma-ray vs. Spin-down Luminosities*

Step 1: express $N_\gamma^{\text{in}}\tau^{\text{in}}$ and $N_\gamma^{\text{out}}\tau^{\text{out}}$ with $P, \mu, \alpha, T, h_\text{m}$.

An inward e$^-$ or an outward e$^+$ emits

$$(N_\gamma)^{\text{in}} = eE_{\|} l_2 / h\nu_c, \quad (N_\gamma)^{\text{out}} = eE_{\|} l_1 / h\nu_c$$

photons while running the distance l_2 or l_1.

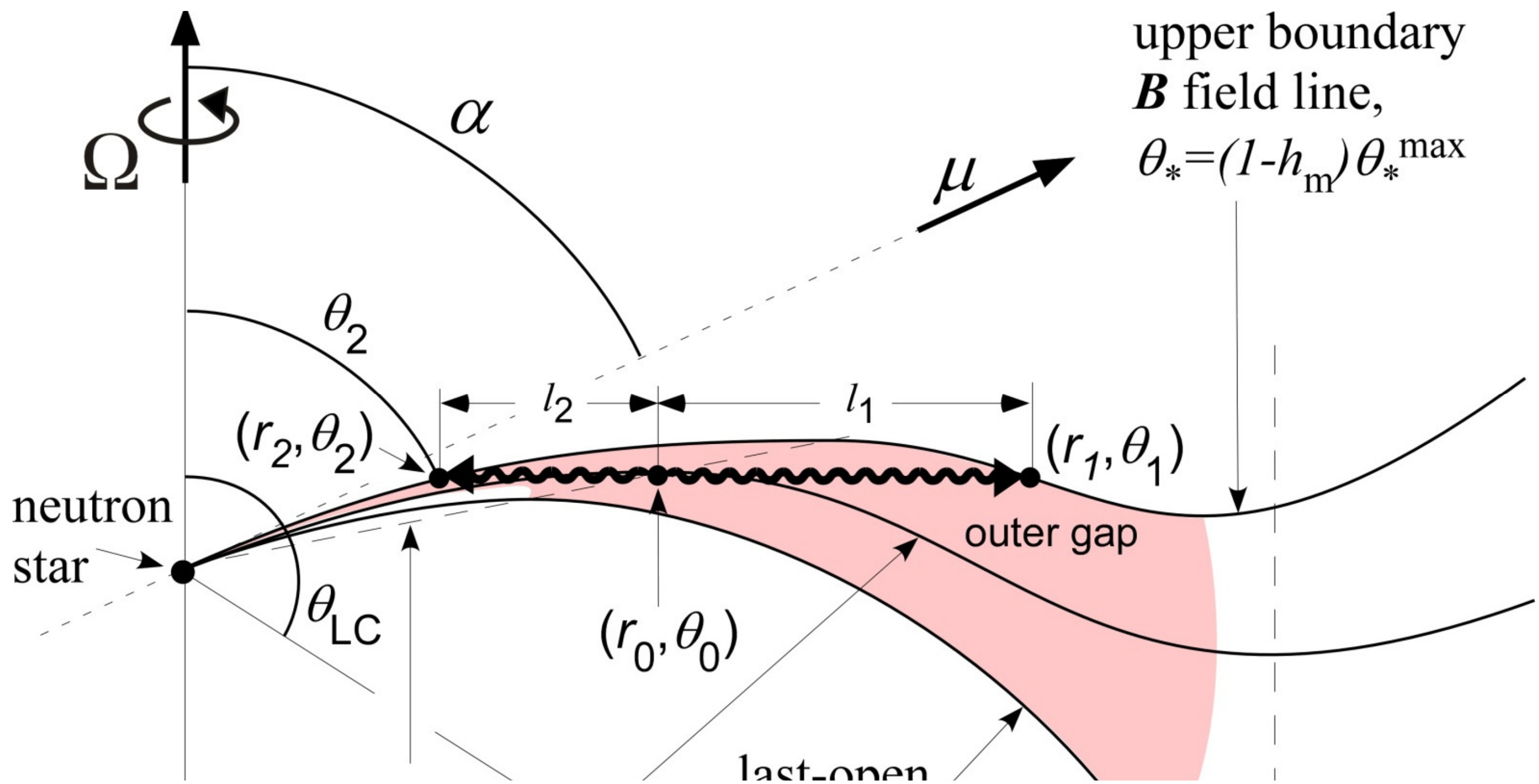

§4 Gamma-ray vs. Spin-down Luminosities

Step 1: express $N_\gamma^{\text{in}}\tau^{\text{in}}$ and $N_\gamma^{\text{out}}\tau^{\text{out}}$ with P, μ, α, T, h_{m}.

An inward e^- or an outward e^+ emits

$$(N_\gamma)^{\text{in}} = eE_{\|} l_2 / h\nu_c, \quad (N_\gamma)^{\text{out}} = eE_{\|} l_1 / h\nu_c$$

photons while running the distance l_2 or l_1.

Such photons materialize as pairs with probability

$$\tau^{\text{in}} = l_2 F_2 \sigma_2 / c, \quad \tau^{\text{out}} = l_1 F_1 \sigma_1 / c$$

where F_1, F_2 denotes the X-ray flux and σ_1, σ_2 the pair-production cross section.

Quantities l_1, l_2, F_1, F_2, σ_1, σ_2 can be expressed by P, μ, α, T, and h_{m}, if we specify the ***B*** field configuration.

§4 Gamma-ray vs. Spin-down Luminosities

Step 1: Both $N_\gamma^{\mathrm{in}}\tau^{\mathrm{in}}$ and $N_\gamma^{\mathrm{out}}\tau^{\mathrm{out}}$ are expressed in terms of P,μ,α,T, and h_{m}. Thus, $N_\gamma^{\mathrm{in}}\tau^{\mathrm{in}} N_\gamma^{\mathrm{out}}\tau^{\mathrm{out}}=1$ gives $h_{\mathrm{m}} = h_{\mathrm{m}}(P,\mu,\alpha,T)$.

Step 2: Specifying the spin-down law, $P=P(t,\alpha)$, and the cooling curve, $T=T(t)$, we can solve $h_{\mathrm{m}} = h_{\mathrm{m}}(t, \alpha)$.

Step 3: Independently, $P=P(t,\alpha)$ gives $\dot{E} = \dot{E}(t,\alpha)$.

Step 4: Therefore, we can relate

$$\mathrm{L}_\gamma = \mathrm{L}_\gamma(t,\alpha) \propto h_{\mathrm{m}}{}^3\, \dot{E}$$

and

$$\dot{E} = \dot{E}(t,\alpha)$$

with intermediate parameter, pulsar age, t.

§4 *Gamma-ray vs. Spin-down Luminosities*

Step 2: Give spin-down law and NS cooling curve.

Assume dipole-radiation formula,

$$-I\Omega\dot{\Omega} = \frac{2}{3}\frac{\mu^2\Omega^4}{c^3} \quad \rightarrow \; P = P(t,\alpha)$$

Adopt the minimum cooling scenario (i.e., without any direct-Urca, rapid cooling processes).

$$\rightarrow \; T = T(t)$$

§4 Gamma-ray vs. Spin-down Luminosities

Step 2: Cooling curves in the minimum cooling scenario:

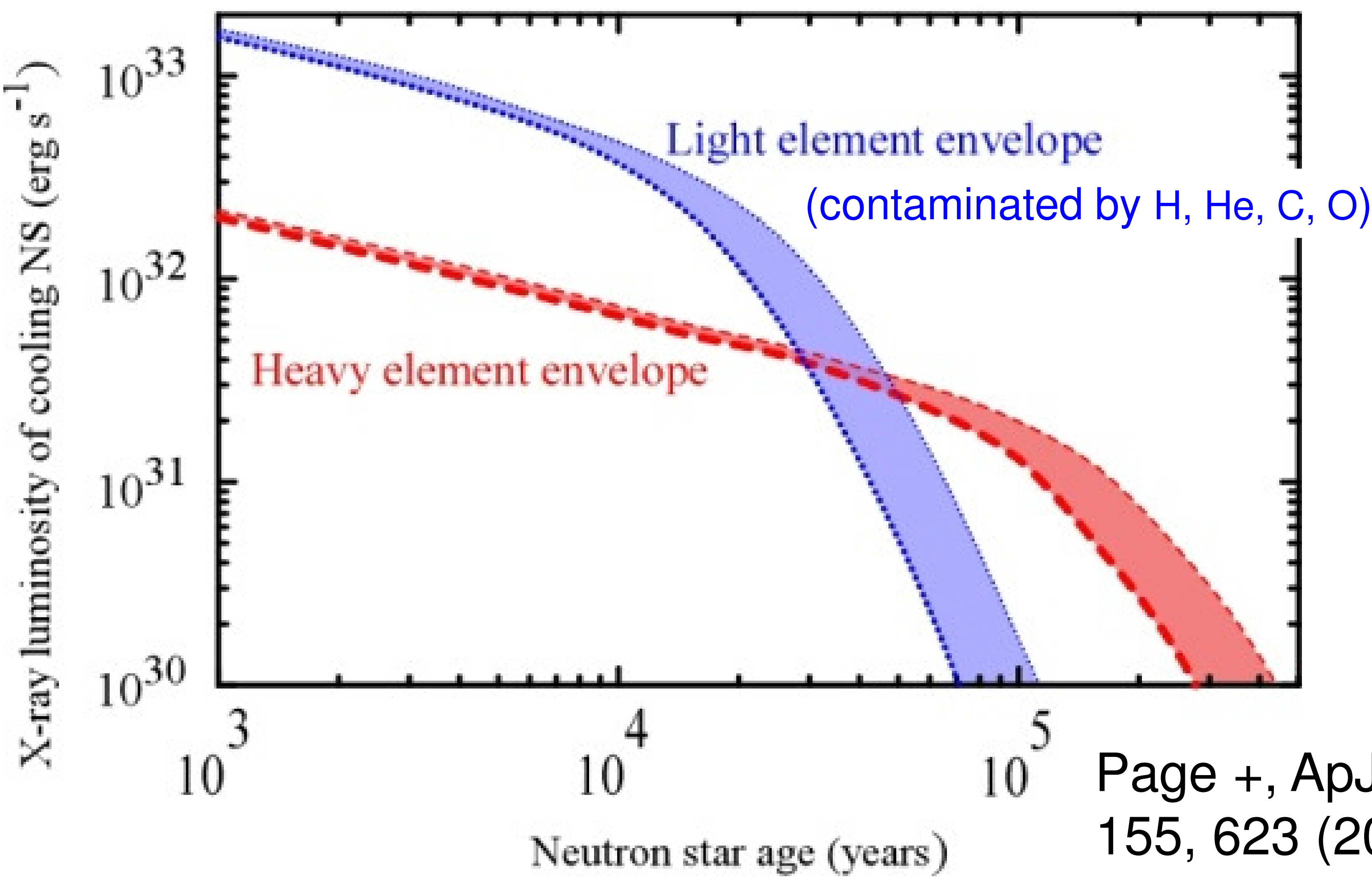

Page +, ApJS 155, 623 (2004)

Step 2: Now we can solve $h_m = h_m(t)$.

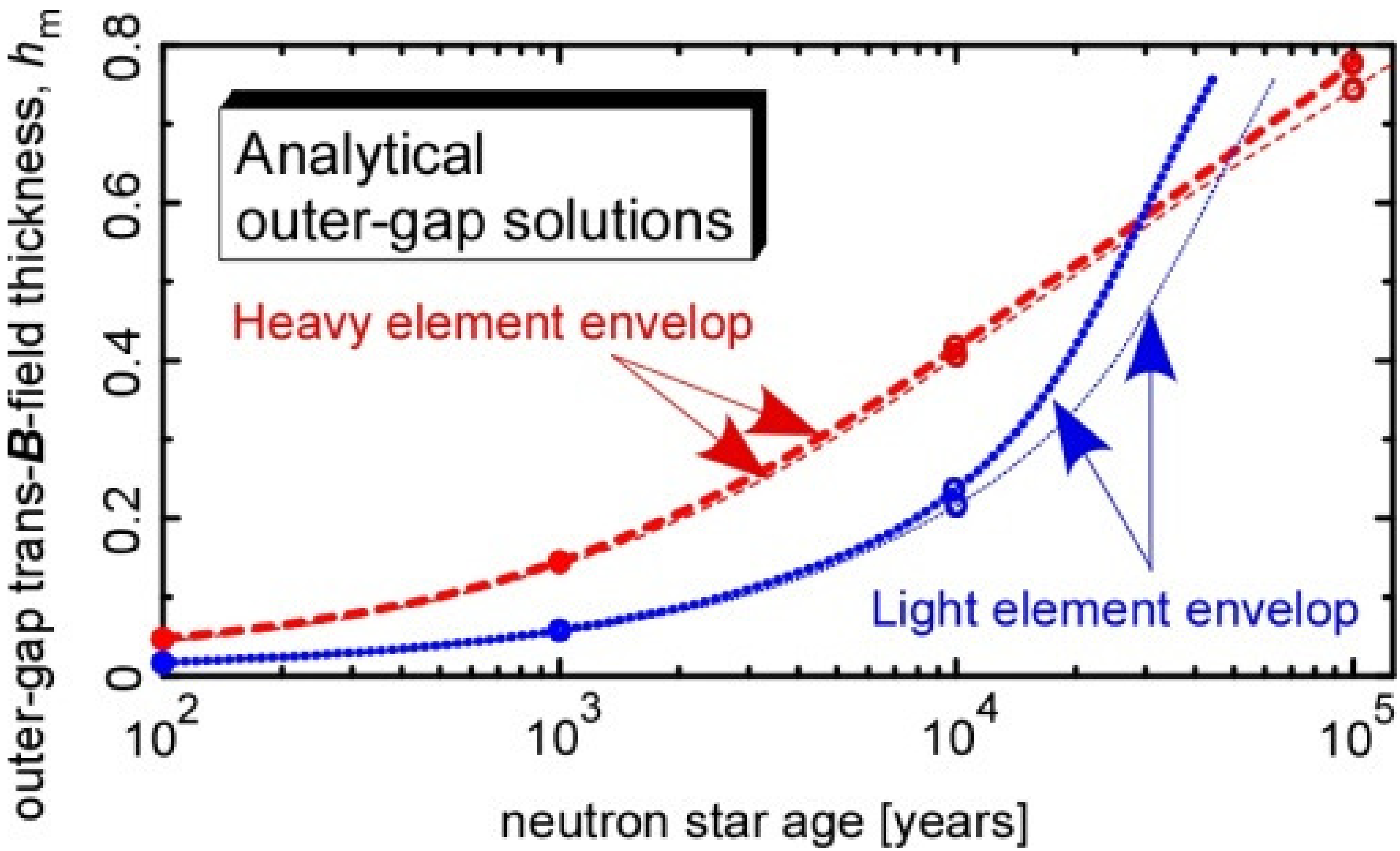

§4 Gamma-ray vs. Spin-down Luminosities

Step 1: Both $N_\gamma^{\rm in}\tau^{\rm in}$ and $N_\gamma^{\rm out}\tau^{\rm out}$ are expressed in terms of P, μ, α, T, and $h_{\rm m}$. Thus, $N_\gamma^{\rm in}\tau^{\rm in} N_\gamma^{\rm out}\tau^{\rm out}=1$ gives $h_{\rm m} = h_{\rm m}(P, \mu, \alpha, T)$.

Step 2: Specifying the spin-down law, $P=P(t, \alpha)$, and the cooling curve, $T=T(t)$, we can solve $h_{\rm m} = h_{\rm m}(t, \alpha)$.

Step 3: On the other hand, $P=P(t, \alpha)$ gives $\dot{E} = \dot{E}(t, \alpha)$.

Step 4: Therefore, we can relate

$$L_\gamma = L_\gamma(t, \alpha) \propto h_{\rm m}{}^3 \dot{E}$$

and

$$\dot{E} = \dot{E}(t, \alpha)$$

with intermediate parameter, pulsar age, t.

§4 Gamma-ray vs. Spin-down Luminosities

Step 3: We can immediately solve $\dot{E} = \dot{E}(t, \alpha)$ by the spin-down law.

$$\underbrace{\dot{E} = -I\Omega\dot{\Omega} = C(\alpha)\frac{\mu^2\Omega^4}{c^3}}$$

$$\rightarrow \Omega = \Omega(t, \alpha)$$

$$\rightarrow \boxed{\dot{E} = \dot{E}(t, \alpha)}$$

$$C = \frac{2}{3}\sin^2\alpha \quad \text{for magnetic-dipole spin-down}$$

$$\approx 1 + \sin^2\alpha \quad \text{for force-free spin-down}$$

§4 Gamma-ray vs. Spin-down Luminosities

Step 1: Both $N_\gamma^{\rm in}\tau^{\rm in}$ and $N_\gamma^{\rm out}\tau^{\rm out}$ are expressed in terms of P, μ, α, T, and $h_{\rm m}$. Thus, $N_\gamma^{\rm in}\tau^{\rm in} N_\gamma^{\rm out}\tau^{\rm out}=1$ gives $h_{\rm m} = h_{\rm m}(P,\mu,\alpha,T)$.

Step 2: Specifying the spin-down law, $P=P(t,\alpha)$, and the cooling curve, $T=T(t)$, we can solve $h_{\rm m} = h_{\rm m}(t, \alpha)$.

Step 3: On the other hand, $P=P(t,\alpha)$ gives $\dot{E} = \dot{E}(t,\alpha)$.

Step 4: Therefore, we can relate

$$\mathrm{L}_\gamma = \mathrm{L}_\gamma(t,\alpha) \propto h_{\rm m}{}^3\,\dot{E}$$

and

$$\dot{E} = \dot{E}(t,\alpha)$$

with intermediate parameter, pulsar age, t.

§4 Gamma-ray vs. Spin-down Luminosities

Step 4: Use $h_m = h_m(t)$ to relate $L_\gamma \propto h_m^{\ 3} \dot{E}$ with $\dot{E} = \dot{E}(t)$.

Analytical outer-gap solutions

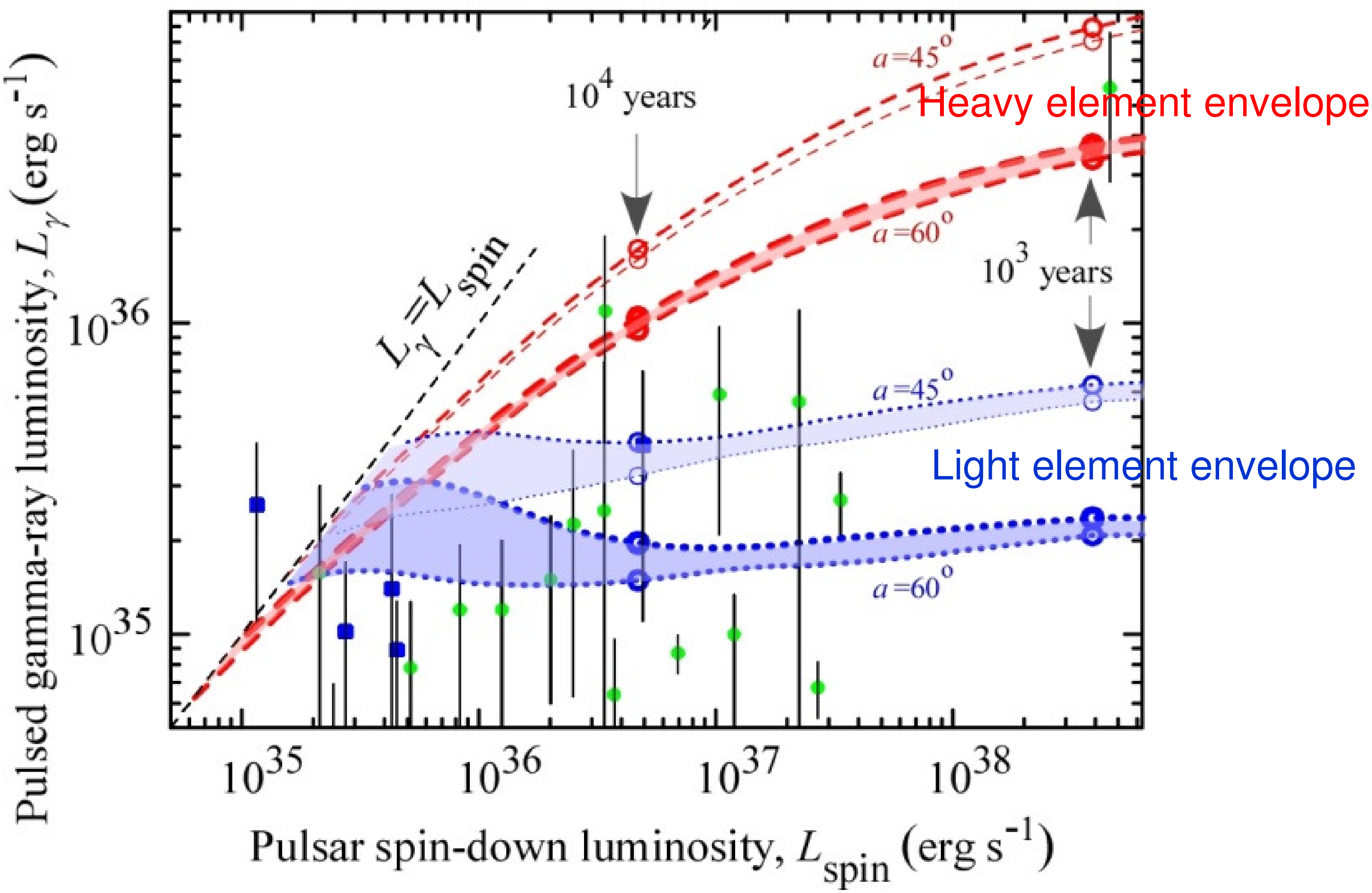

§4 Gamma-ray vs. Spin-down Luminosities

Numerical solution is consistent with the analytical one.

$L\gamma \sim L_{spin}{}^{0\text{-}0.4}$
if $L_{spin} > 10^{36}$ erg/s

However,
$L\gamma$ declines rapidly
if $L_{spin} < 10^{35.5}$ erg/s

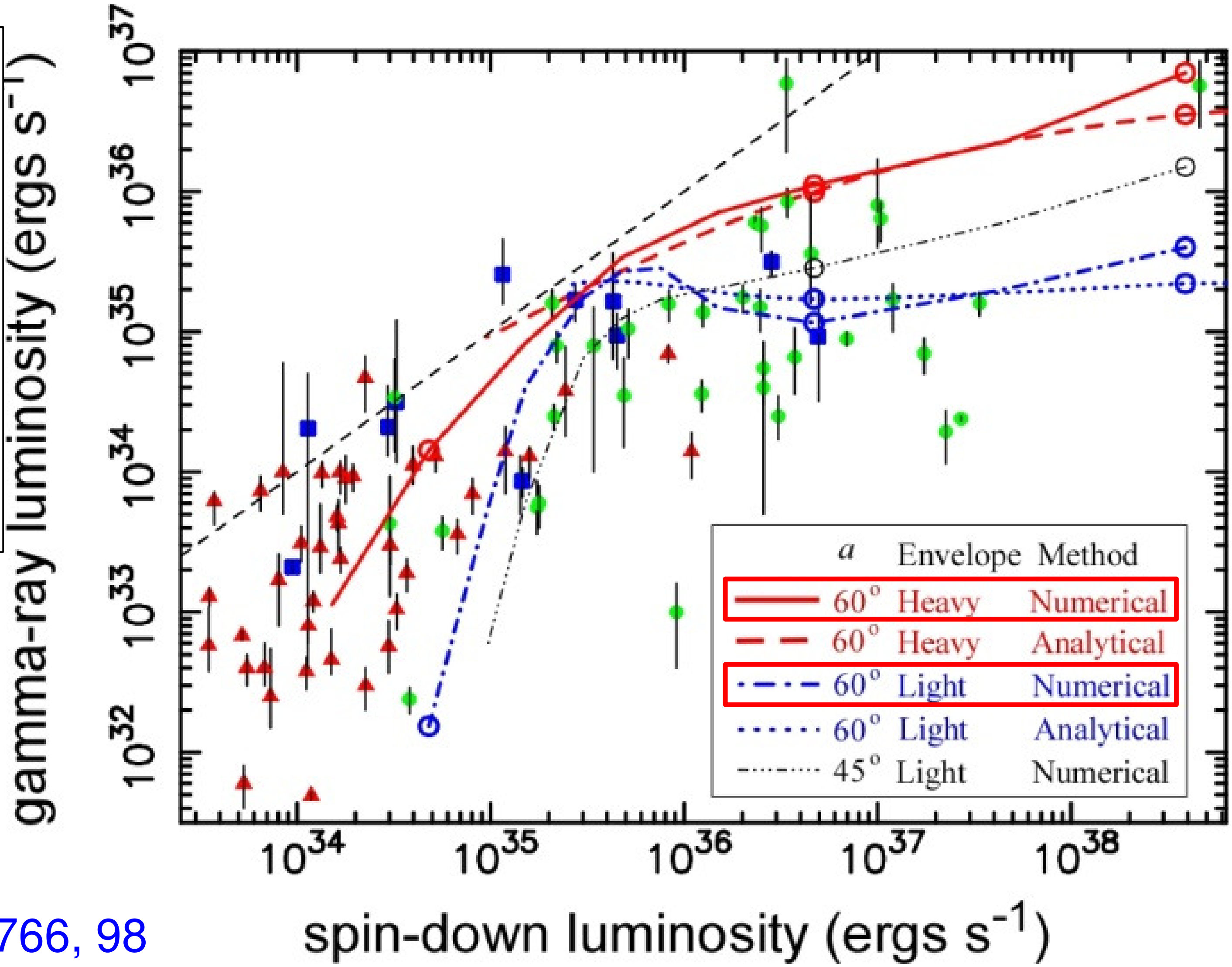

KH (2013) ApJ 766, 98

§4 Gamma-ray vs. Spin-down Luminosities

To convert the observed flux F_γ into luminosity,
$L_\gamma = 4\pi f_\Omega F_\gamma d^2$, it is (conventionally) assumed $f_\Omega = 1$.

However, we **underestimate L_γ if f_Ω>1**.

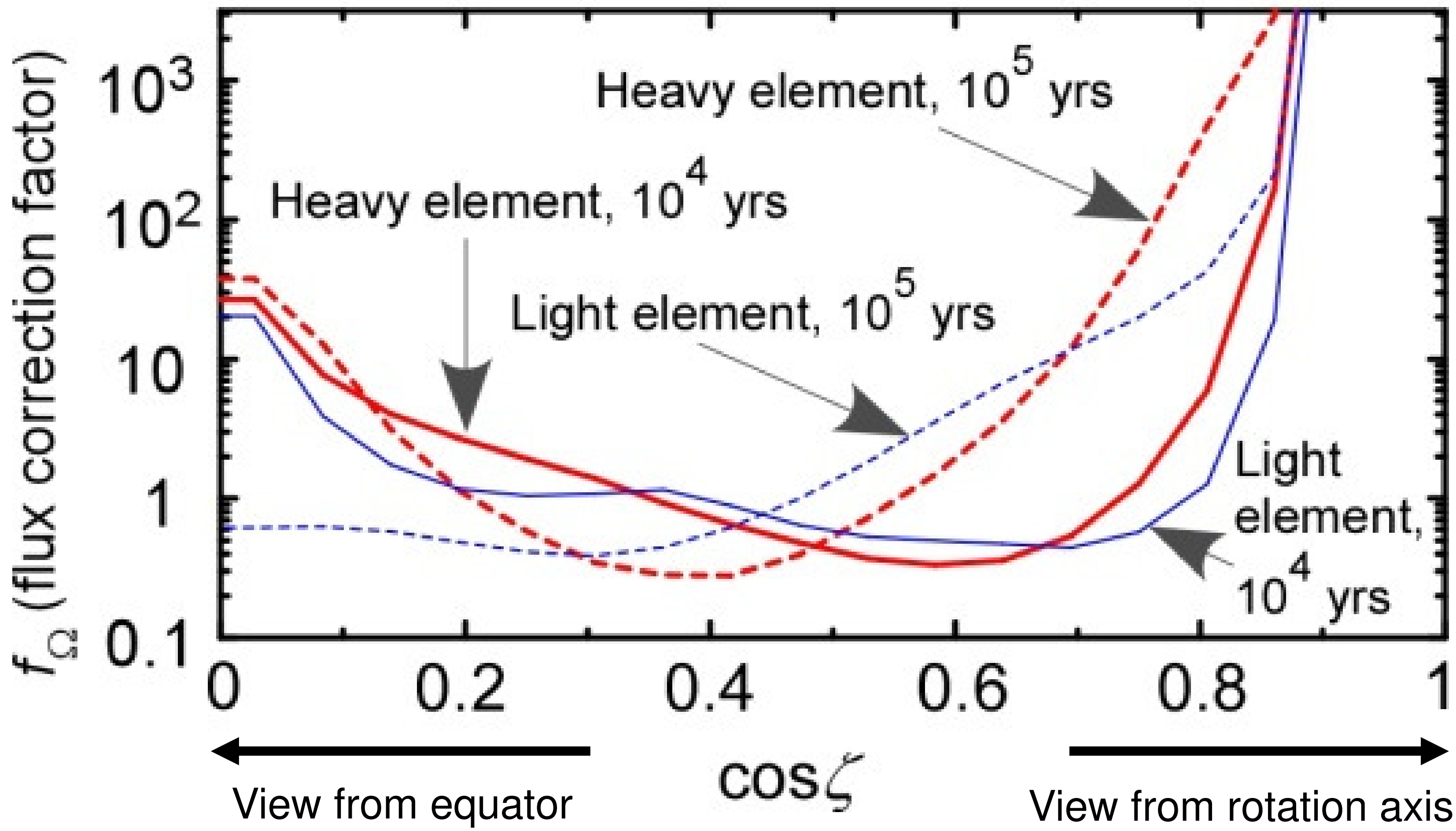

§4 *Gamma-ray vs. Spin-down Luminosities*

To convert the observed flux F_γ into luminosity, $L_\gamma = 4\pi f_\Omega F_\gamma d^2$, it is (conventionally) assumed $f_\Omega = 1$.

For example, **we obtain $f_\Omega > 3$ with probability ~50%.**

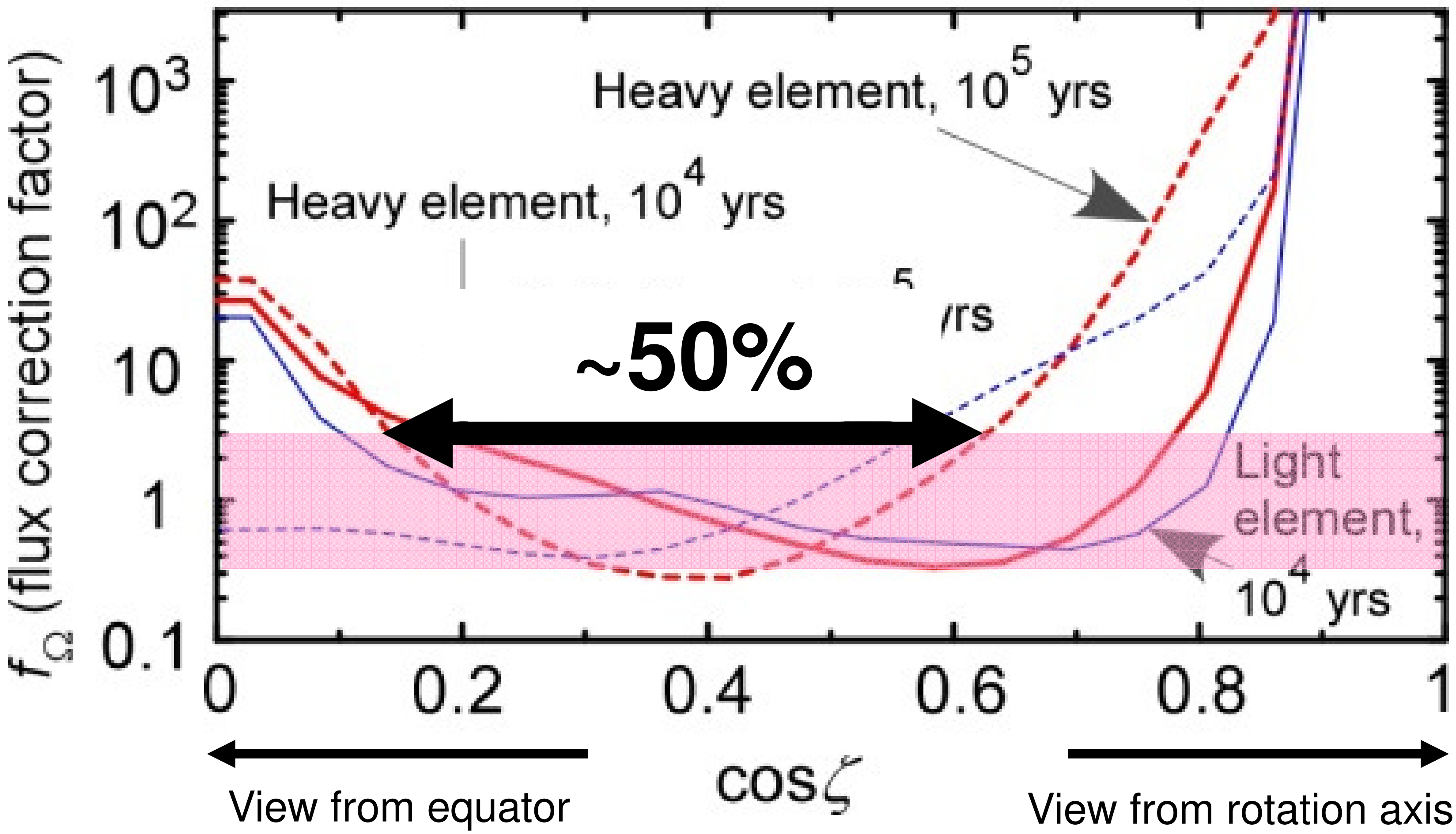

§4 Gamma-ray vs. Spin-down Luminosities

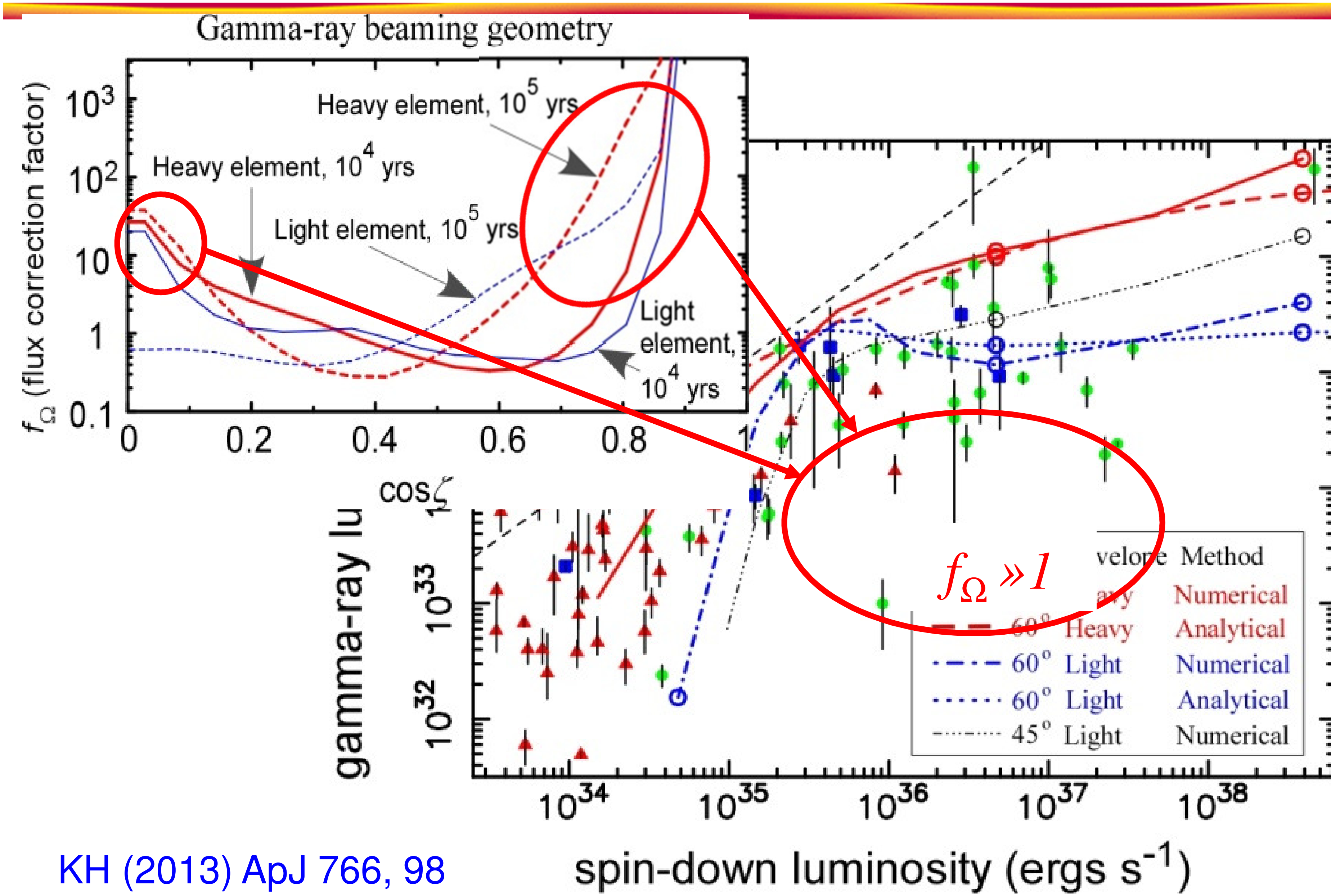

KH (2013) ApJ 766, 98

§5 Application to the Crab pulsar

We can apply the same numerical scheme to the Crab pulsar.

Today, we assume

- magnetic inclination angle $\alpha = 60^{\circ}$,
- cooling NS surface temperature kT=100eV,
  (consistent with the cooling curve of a heavy-element envelope)

§5 Application to the Crab pulsar

3-D OG distribution: trans-***B*** thickness, $D_\perp$.,
projected on the last-open ***B*** field line surface.

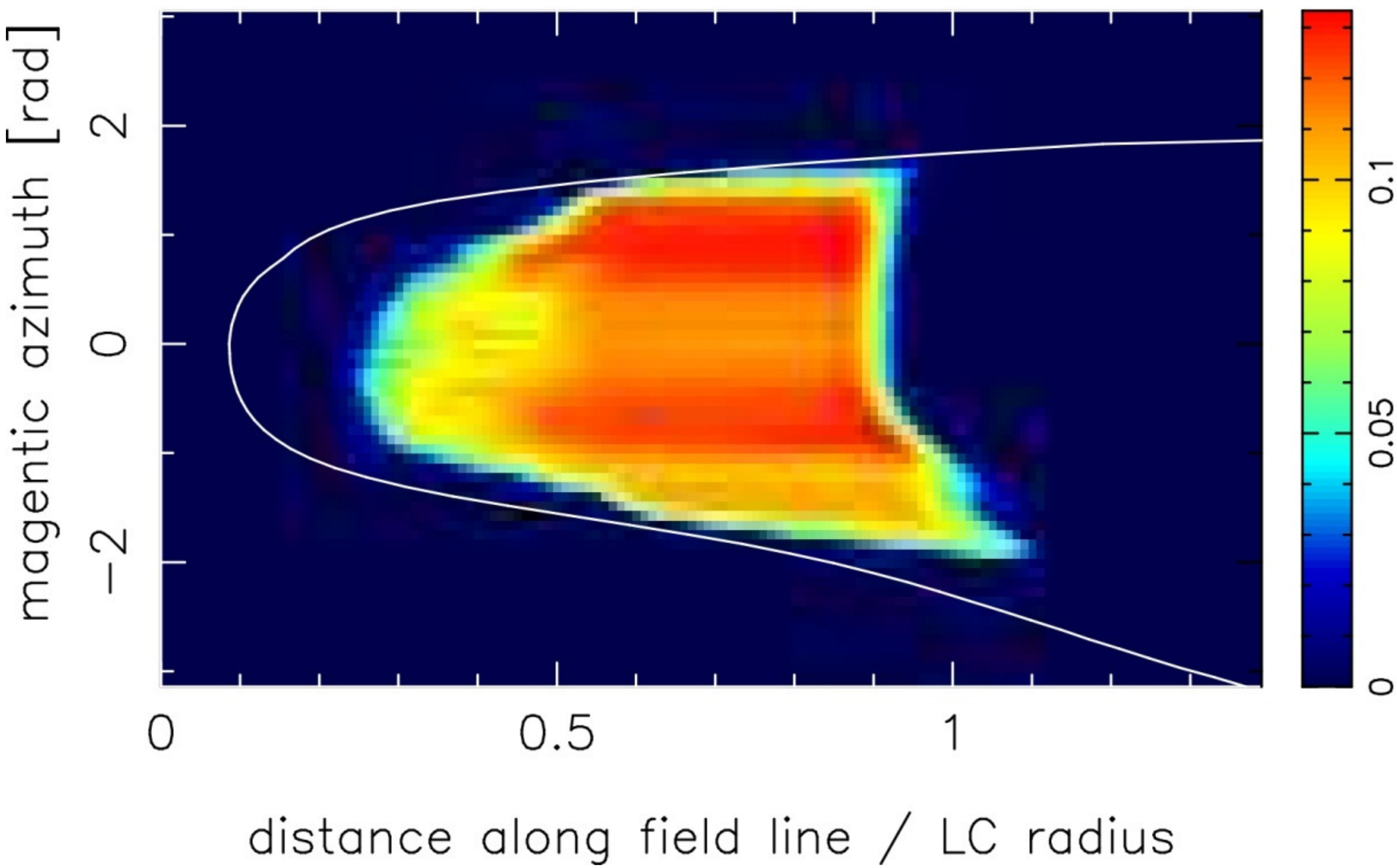

§5 Application to the Crab pulsar

Distribution of acceleration ***E*** field, $E_{||}$.

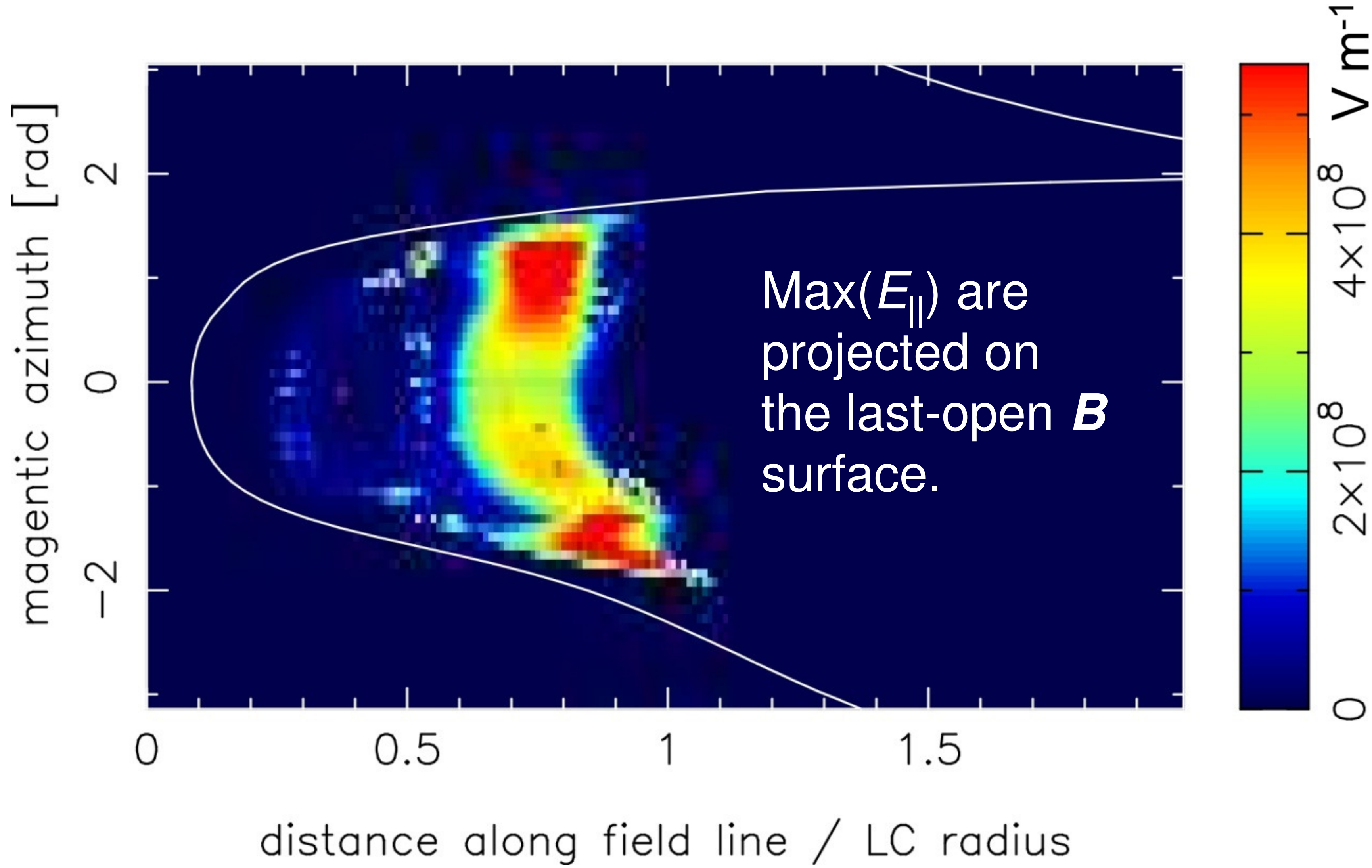

§5 Application to the Crab pulsar

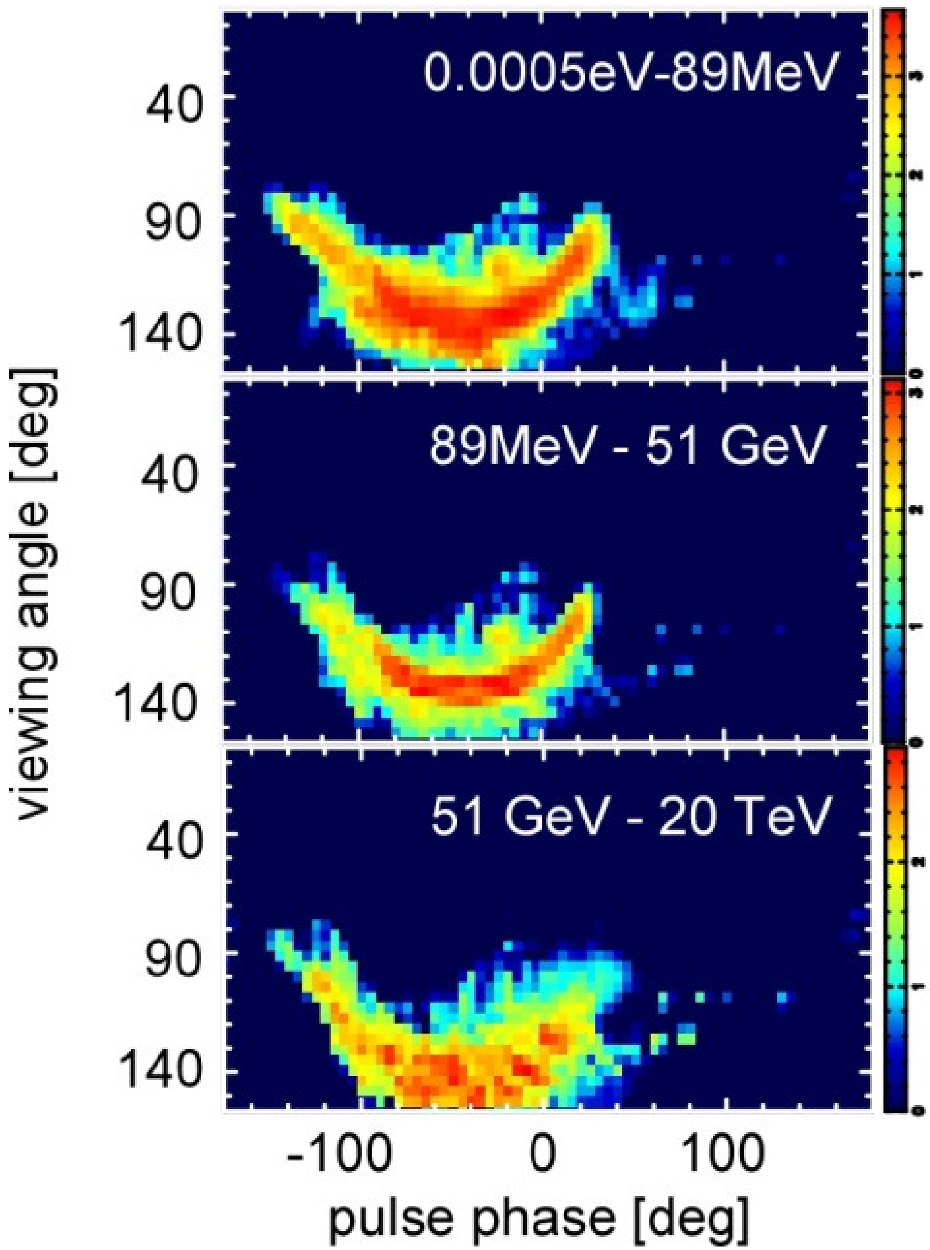

Sky map of OG emission

Secondary/tertiary synchrotron emission

Primary curvature & secondary/tertiary SSC emission

Secondary/tertiary SSC emission

§5 Application to the Crab pulsar

If we cut the sky map at a specific viewing angle, we obtain the pulse profile.

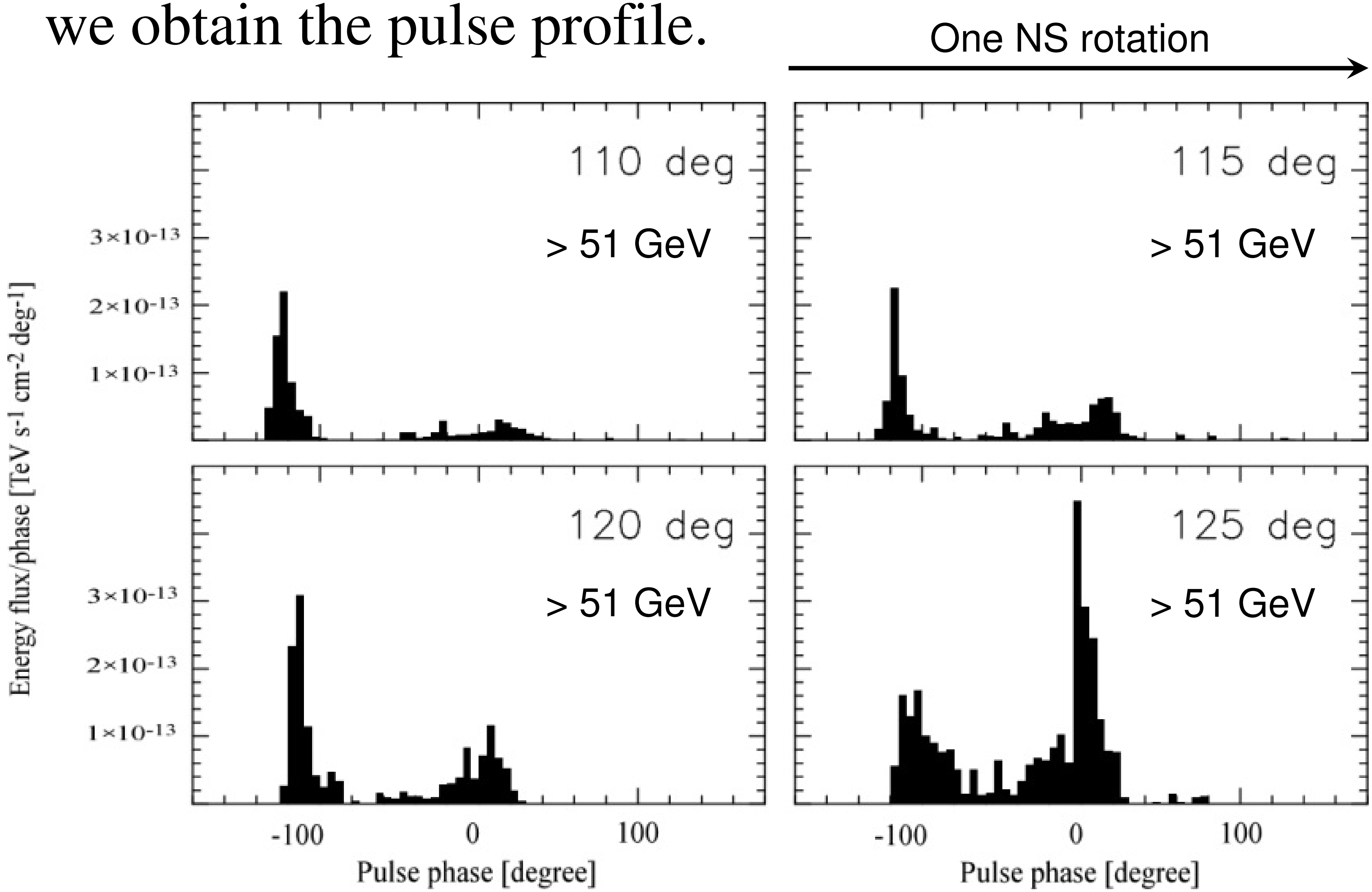

§5 Application to the Crab pulsar

From X-ray observations (of the Crab nebula), $\zeta \sim 120^{\mathrm{o}}$ is suggested.

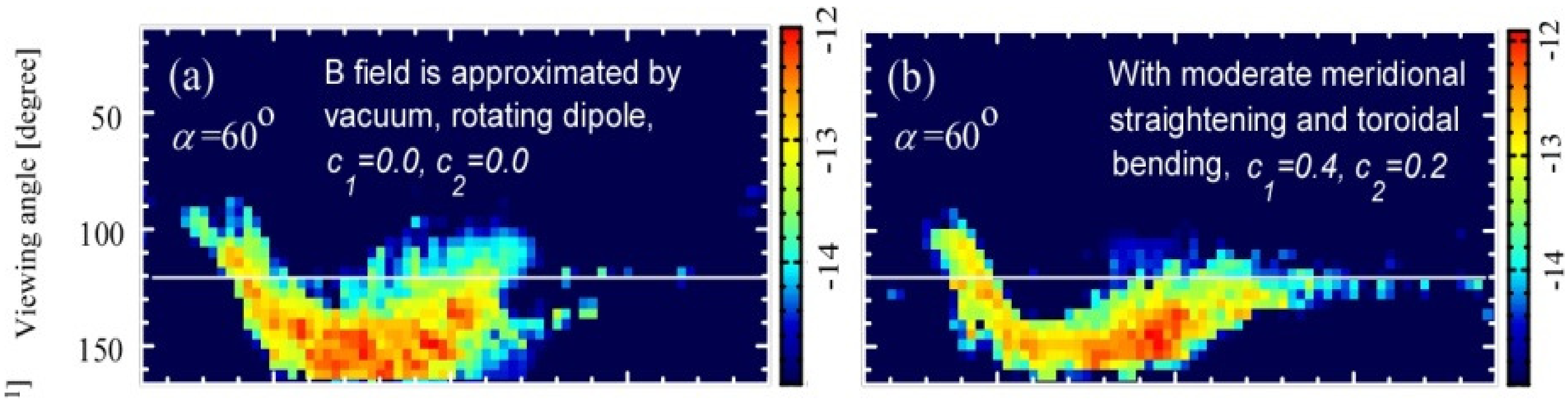

Introduce artificial meridional straightening and toroidal bending of ***B*** field (due to current):

$$B_\theta = (1 - c_1 \varpi / \varpi_{\mathrm{LC}}) B_{\theta,\mathrm{vac}}$$

$$B_\phi = (1 + c_2 \varpi / \varpi_{\mathrm{LC}}) B_{\phi,\mathrm{vac}}$$

§5 Application to the Crab pulsar

Peak separation increases if ***B*** field is toroidally bent and meridionally straightened moderately.

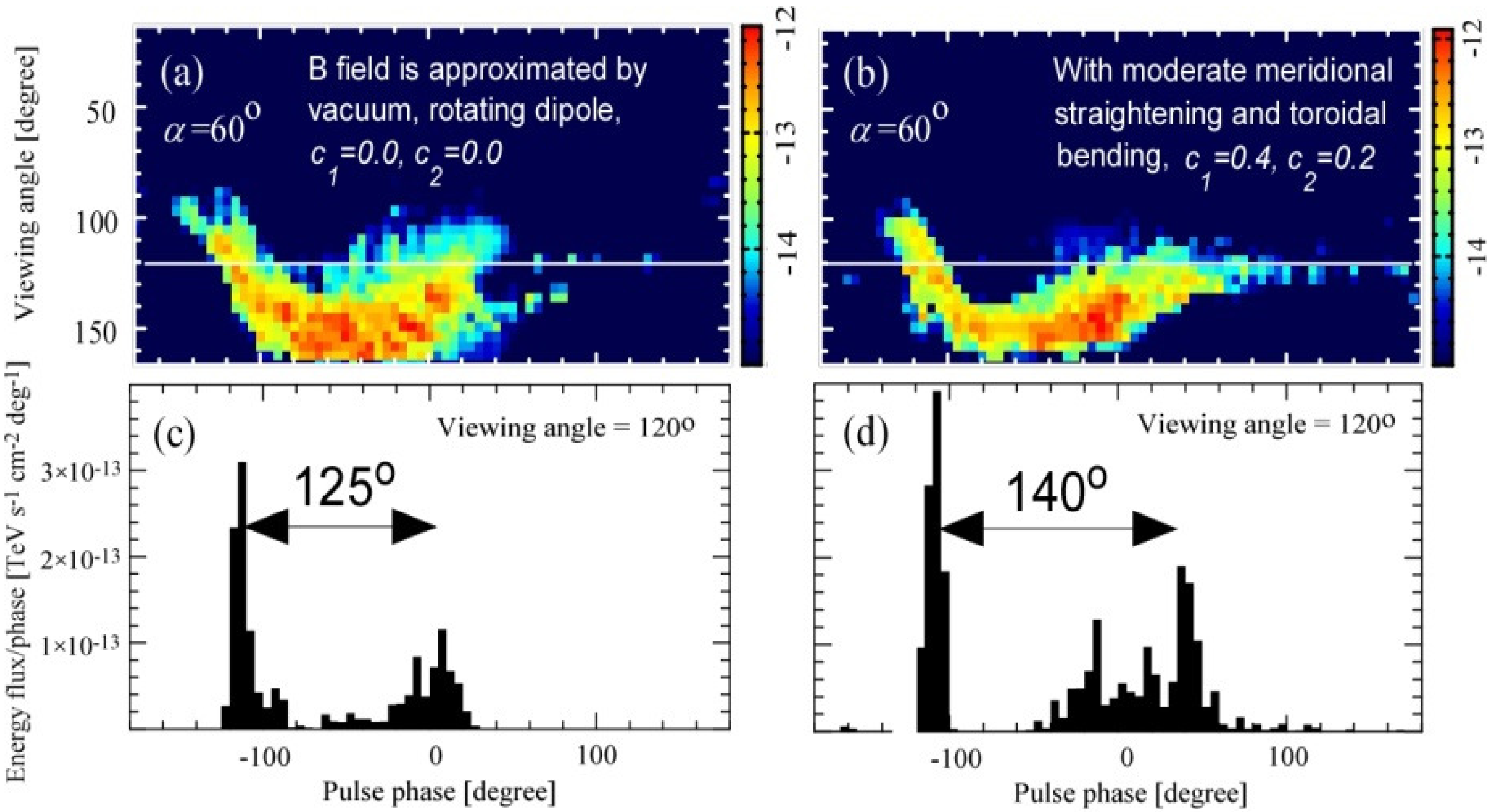

§5 Application to the Crab pulsar

Peak separation increases if ***B*** field is toroidally bent and meridionally straightened moderately.

We can in principle discriminate ***B* field structure near the LC**, which has been highly unknown.

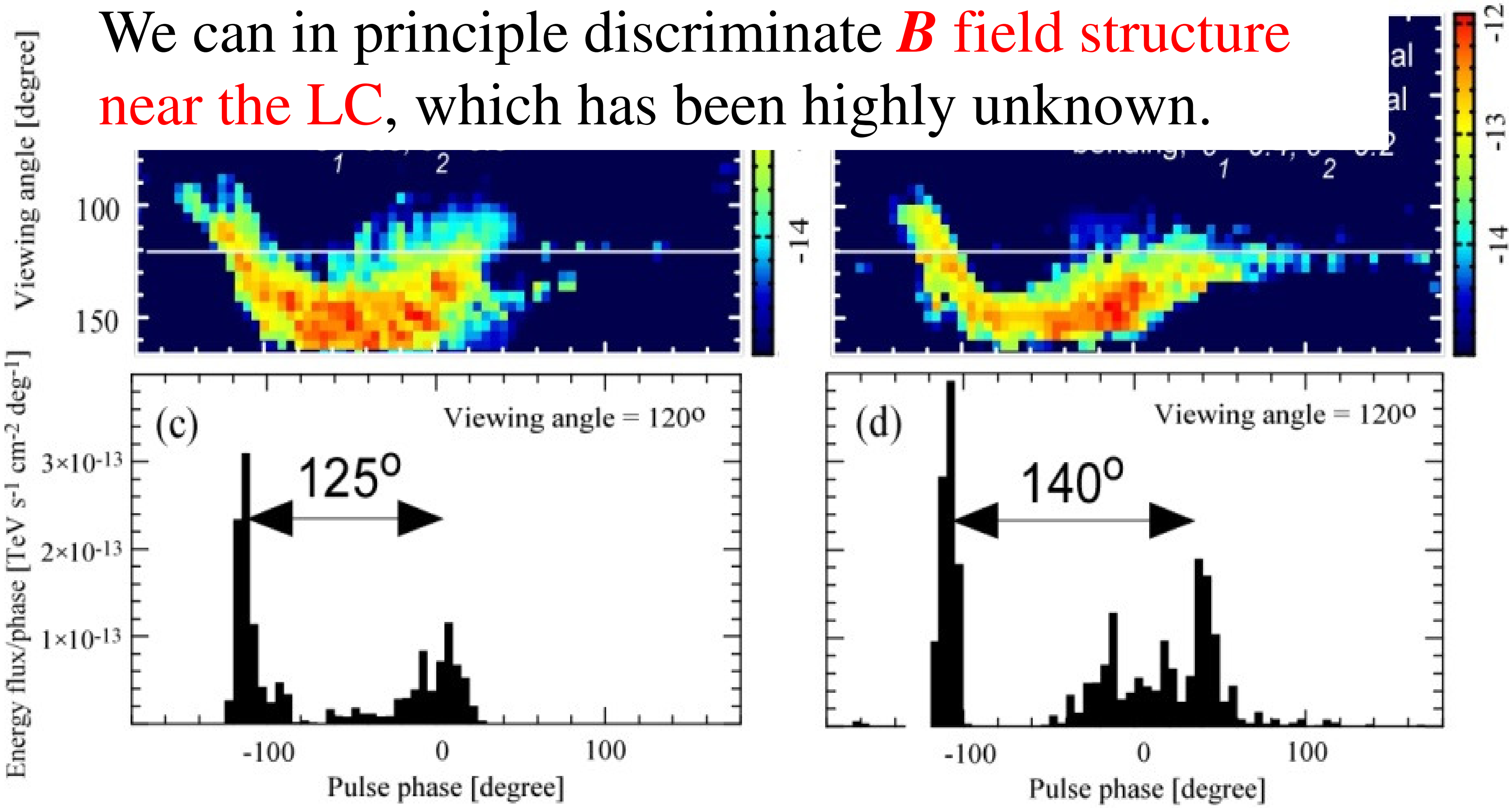

§5 *Application to the Crab pulsar*

Schematic picture of cascading pairs and their emissions:

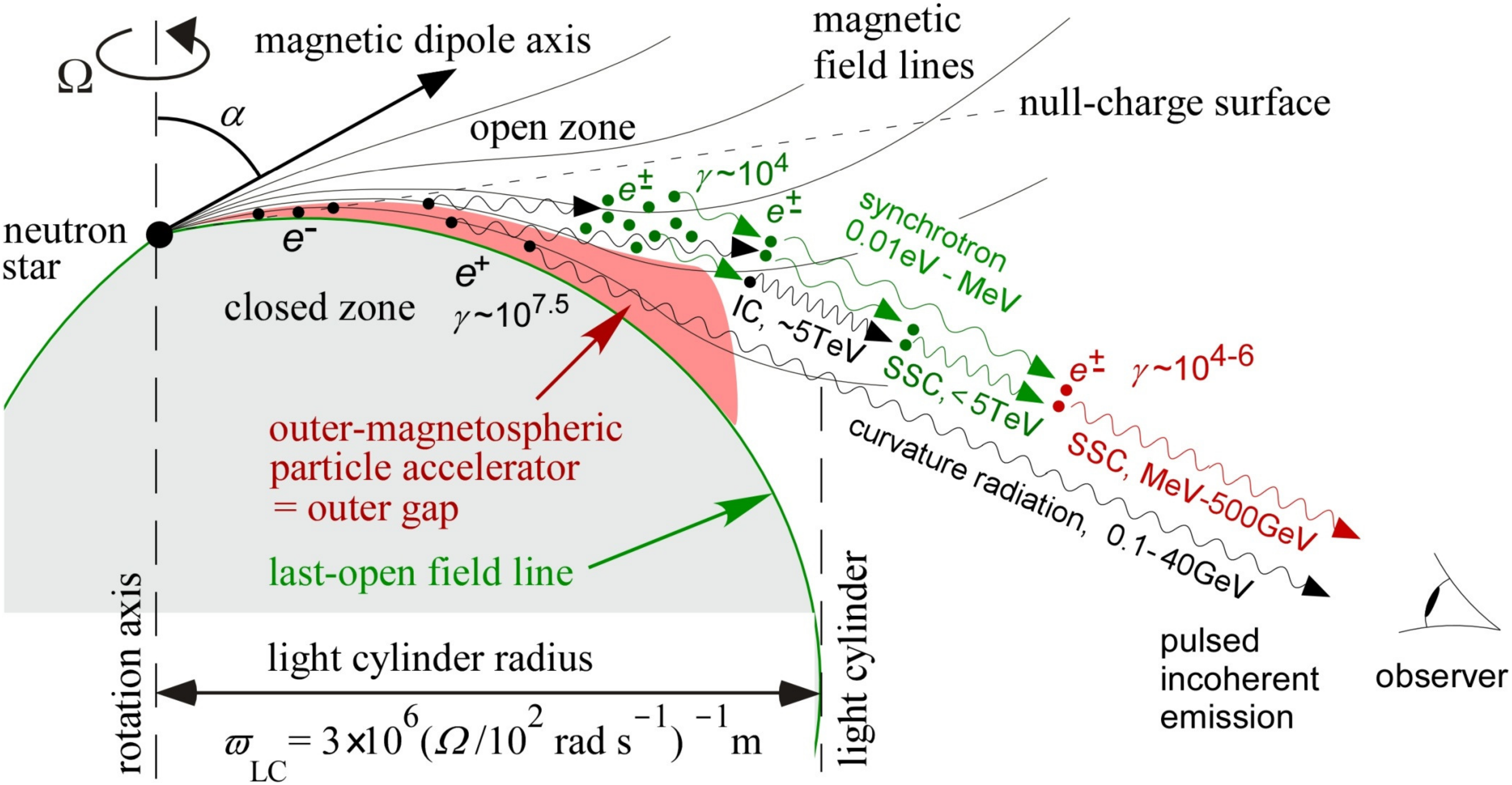

§6 Lorentz invariance violation tests

Finally, let us consider the Lorentz invariance violation tests using pulsars.

Quantum gravity can be tested e.g., by measuring an energy-dependent dispersion relation of mass-less particles.

Ex.) Photons would propagate at the speed

$$\frac{v(E)}{c} = 1 \pm \left(\frac{E}{E_{QG}} \right)^n$$

For $n=1$, for instance, two photons with different energies E_1 and E_2 will arrive with time difference,

$$\Delta t = \frac{L}{c} \frac{E_2 - E_1}{E_{\mathrm{QG}}}$$

§6 Lorentz invariance violation tests

$$\Delta t = \frac{L}{c}\frac{E_2 - E_1}{E_{\mathrm{QG}}} \quad \text{or} \quad E_{\mathrm{QG}} = \frac{L}{c}\frac{E_2 - E_1}{\Delta t}$$

If two photons are emitted at the same place (i.e., same L), we can derive E_{QG} (or set a lower bound of E_{QG}) from Δt.

Shot-time events (small Δt) with large photon-energy separation (greater E_2-E_1) are ideal.

§6 Lorentz invariance violation tests

They applied this method to rotation-powered pulsars and examined *Δt* at different photon energies, assuming that GeV and TeV photons are emitted from the same location in the magnetosphere.

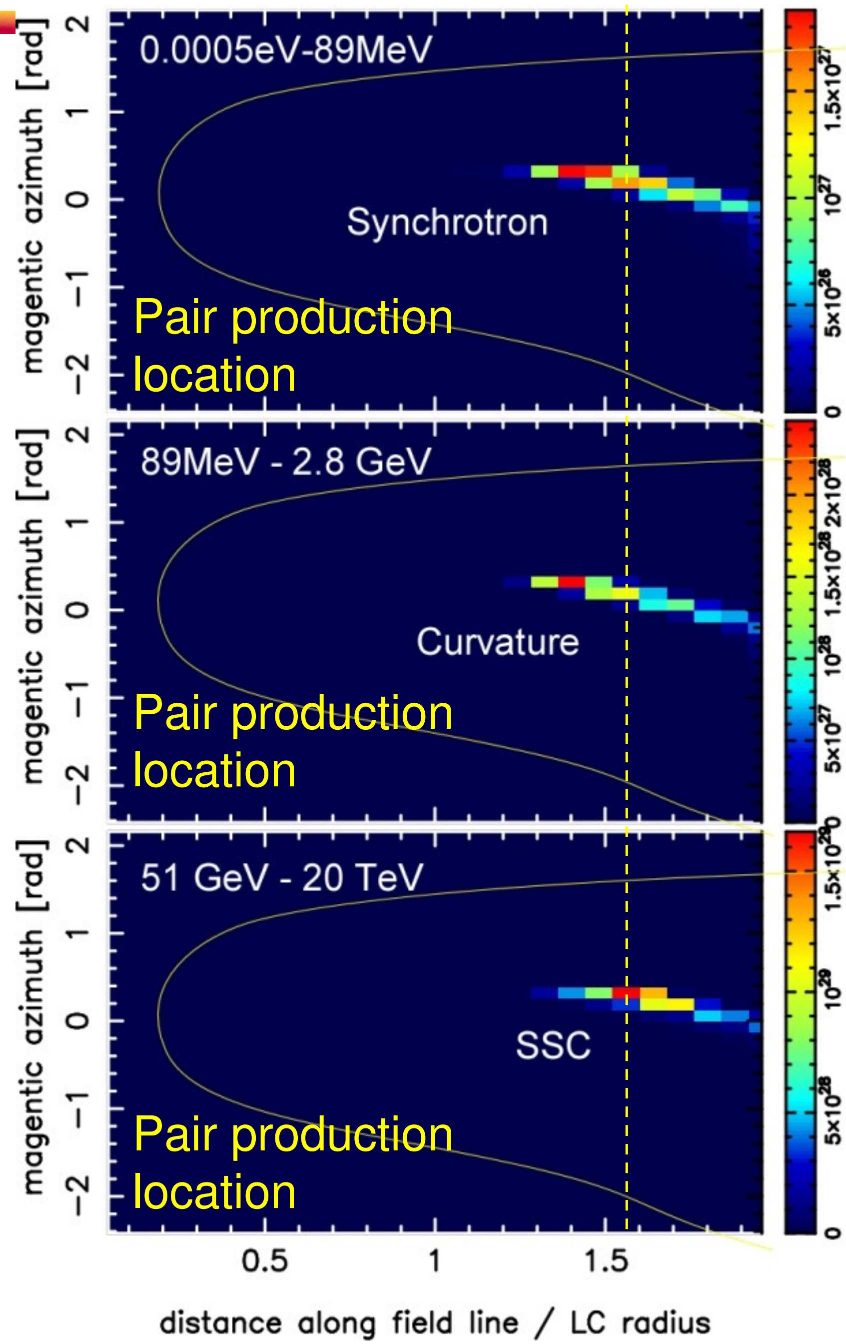

See e.g.,

Zitzer +, ICRC2013, Rio de Janeiro

Otte, ICRC, Beijing

McCann +, 4th Fermi sympo, Monteley

§6 *Lorentz invariance violation tests*

They applied this method to rotation-powered pulsars and examined *Δt* at different photon energies, assuming that GeV and TeV photons are emitted from the same location in the magnetosphere.

However, higher energy photons are emitted from higher altitudes by different emission mechanisms.

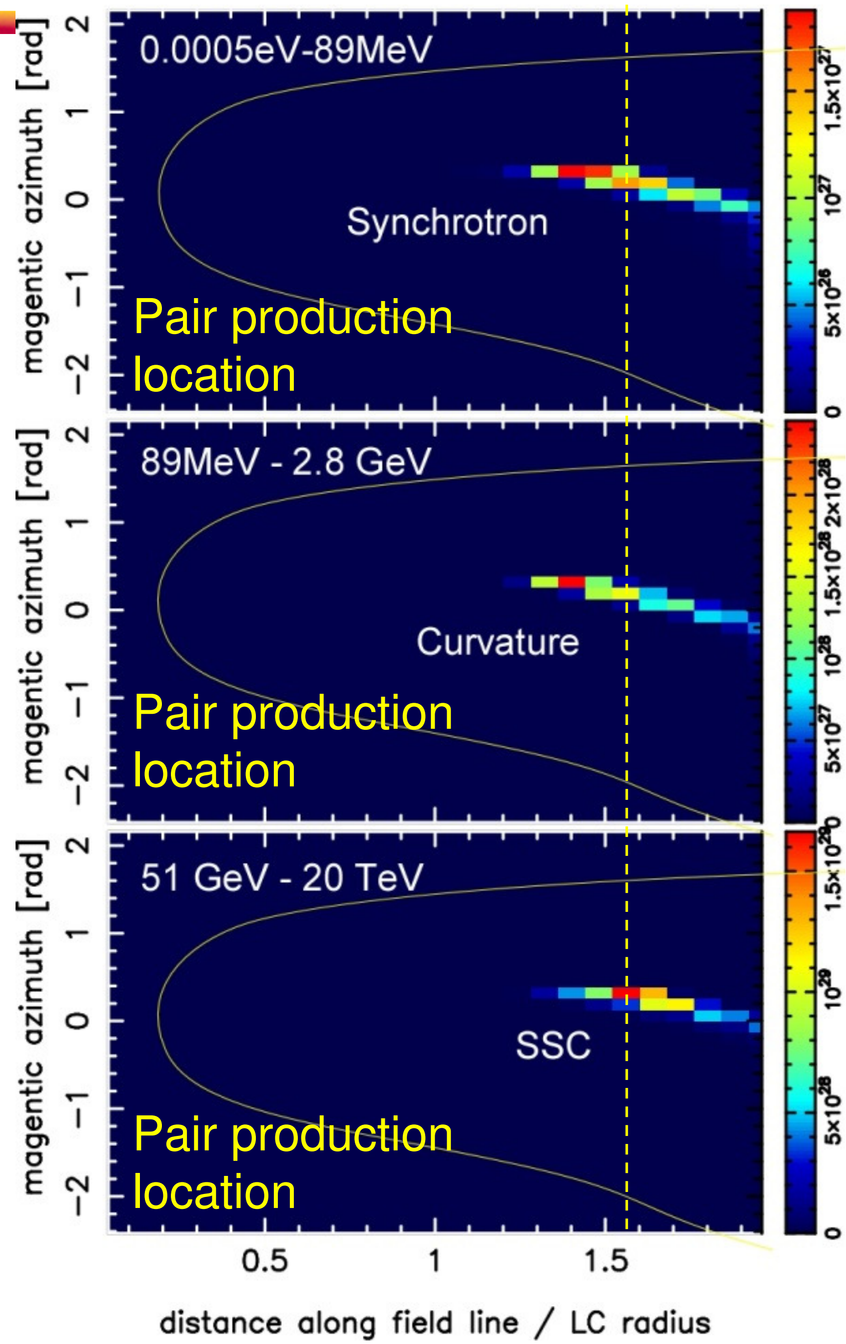

§6 Lorentz invariance violation tests

Indeed, curvature photons and SSC ones appear close in phase.

However, if they appear in different phases, it may merely mean that they are emitted from different locations in the magnetosphere.

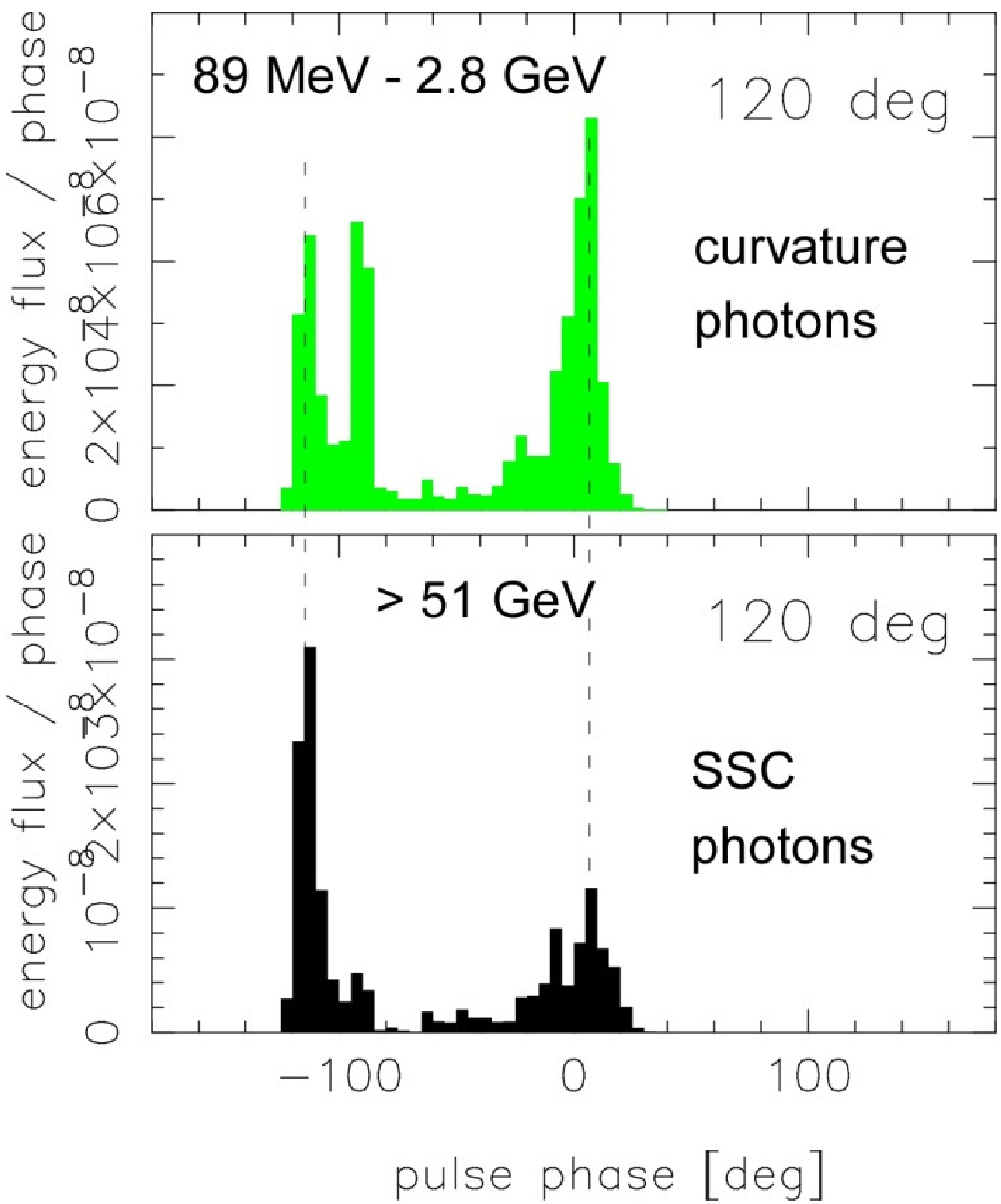

§6 Lorentz invariance violation tests

For example, is ***B*** field is moderately bent toroidally in the counter-rotation direction, HE and VHE pulses will arrive at different phase.

This has nothing to do with the LIV.

$$B_\theta = (1 - c_1 \varpi / \varpi_{\rm LC}) B_{\theta,\rm vac}$$

$$B_\phi = (1 + c_2 \varpi / \varpi_{\rm LC}) B_{\phi,\rm vac}$$

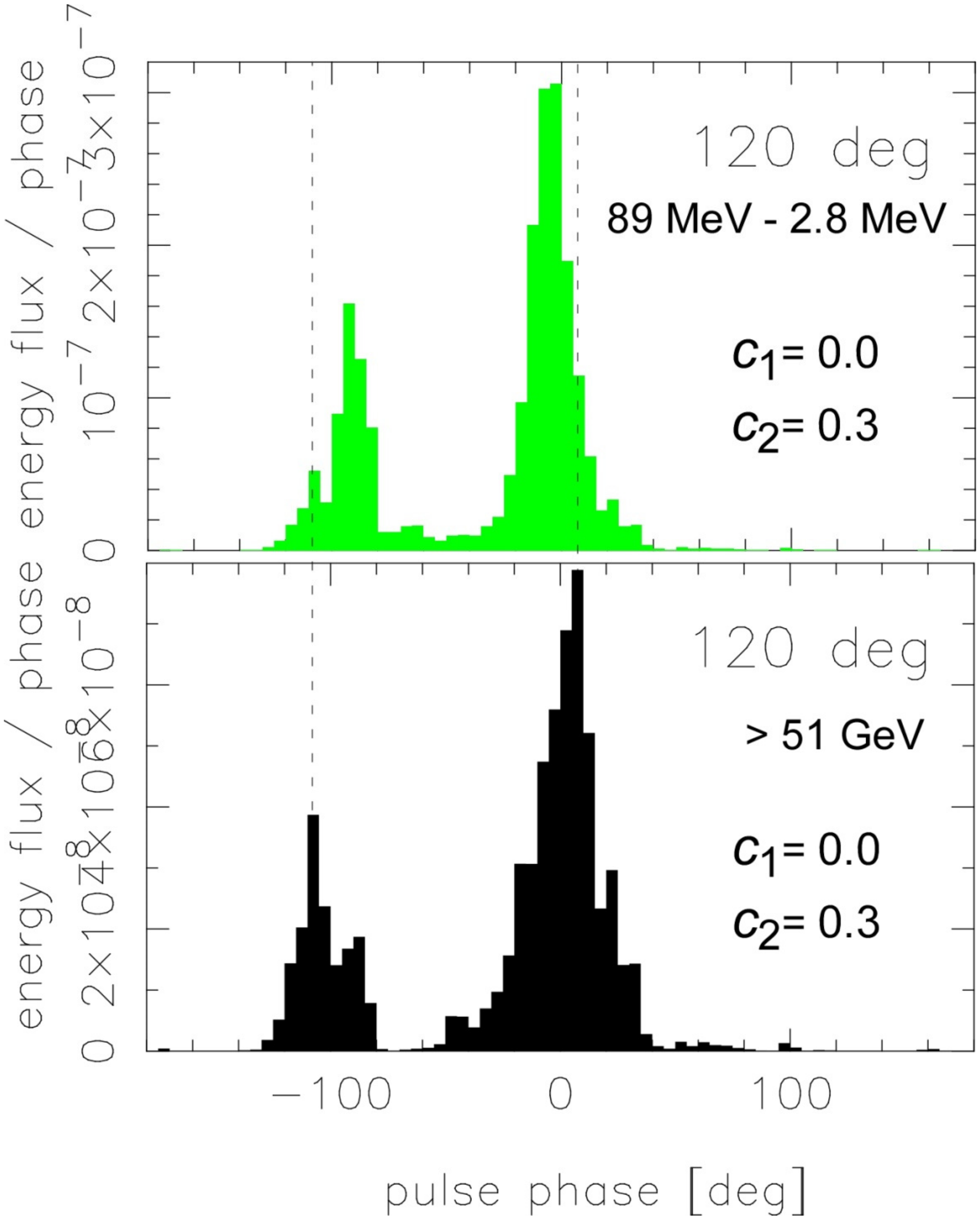

Summary

- High-energy pulsar observations have made rapid progress in recent five years by the advent of Fermi/LAT.
- Development of pulsar emission theory is highly required.
- Now we can predict the HE emissions from pulsar outer magnetospheres, by solving the set of Maxwell ($\mathrm{div}\boldsymbol{E}=4\pi\rho$) and Boltzmann eqs., if we specify P, dP/dt, α_{incl}, kT_{NS}.
- The solution coincidentally corresponds to a quantitative extension of classical outer gap model. However, we no longer have to assume the gap geometry, $E_{||}$, $e^{\pm}$ distribution functions.
- γ-ray luminosity evolves as $L_\gamma \propto \dot{E}^{0-0.4}$ when $\dot{E} > 10^{36.5}$ erg s^{-1}, which is consistent with Fermi/LAT observations.
- Crab pulsar's phase-resolved spectrum can be explained by the current outer-magnetospheric accelerator theory.

Thank you.